The Origins and Further Development of the Jameson-Schmidt-Turkel (JST) Scheme

Antony Jameson*
Department of Aeronautics and Astronautics, Stanford University, Stanford, CA, 94305

This paper is in response to an invitation to give a presentation on the origins and subsequent development of the Jameson-Schmidt-Turkel scheme. After a description of the historical background and initial development of the scheme, the paper discusses three main developments: first, the development of convergence acceleration methods, including residual averaging and multigrid; second, the extension to unstructured grids; and third the reformulation of the JST scheme as a total variation diminishing (TVD) scheme, and its relationship to symmetric TVD schemes. The paper concludes with a brief review of applications to unsteady and viscous flows.

I. Introduction

This paper is in response to an invitation to give a presentation on the origins and subsequent development of the Jameson-Schmidt-Turkel (JST) scheme in a session on history at the Aviation 2015 meeting in Dallas, Texas. The JST scheme was presented at the AIAA 14th Fluid and Plasma Dynamics Conference in Palo Alto, CA, June 1981 as AIAA Paper 81-1259. This paper has been widely cited, but it was never submitted for publication as a journal article, primarily because the present author considered it as only the first step in as yet incomplete research to find a definitive method to solve the Euler equations.

Section II. of the paper gives a synopsis of the origins and goals of the JST scheme, which immediately proved to be successful in a wide variety of CFD simulations. The next steps were the further improvement of the rate of convergence to a steady state by residual averaging, and the introduction of a full approximation agglomeration multigrid scheme, described in section III., and the extension of the method to treat arbitrarily complex configurations on unstructured tetrahedral meshes, outlined in section IV..

Soon after the original presentation of the JST scheme in 1981, there appeared the seminal papers of Roe[2], in which he proposed a characteristics based flux derived from an elegant linearization, and Harten[1], in which he introduced the concept of total variation diminishing (TVD) schemes for scalar conservation laws. Also, by this time the series of papers by Van Leer[3–7] had brought the pioneering work of Godunov[8] to the attention of the CFD community, and introduced the concept of reconstruction with limiters† for the formulation of higher order accurate non-oscillatory shock capturing schemes. These papers ushered in the era of what the author likes to think of as the "flux wars" (Godunov, Steger-Warming, Roe, Osher, AUSM, HLL, HLLC, CUSP) and the "reconstruction wars" (MUSCL, ENO, WENO, SLIP, minmod limiter, superbee limiter, Van Leer limiter, Van Albada limiter, Venkatakrishnan limiter). Ultimately, one can mix and match flux formulations and reconstruction procedures. In order to ensure that the discrete scheme is TVD for a scalar conservation law, the updated state should be a convex combination of the states at neighboring cells at the previous time step. It turns out that this concept extends to the gas dynamics equations. If the discrete solution is physically realizable in the sense that the pressure and density in each cell are non-negative, and the updated state in each cell is a convex combination of the states in neighboring cells, the updated state will also be physically realizable. Moreover, this property can be proven for some flux vector splitting methods, and also for methods stabilized by scalar diffusion, similar to that used in the JST

*Professor of Engineering, Department of Aeronautics and Astronautics, Stanford University, AIAA Fellow

†The idea of limiters to prevent the formation of new extrema in discreet solutions of the gas dynamics equations was first introduced by Boris and Book in their flux corrected transport (FCT) scheme[9].

scheme. In section V., it is shown that when the JST scheme is applied to a scalar conservation law with an appropriate formulation of a switching function, it is actually a symmetric TVD scheme, which may also be labeled as a symmetric limited positive (SLIP) scheme. It is also shown that the SLIP and JST schemes can be reformulated as second order accurate reconstruction schemes, which can then be combined with any preferred choice of the numerical flux.

While the JST scheme was originally designed for steady state solutions, it works quite well for unsteady flows when it is combined with an appropriate time stepping scheme. This is discussed in section VI., while section VII. presents some examples of the application of the JST scheme to compressible viscous flows, modeled by the Reynolds averaged Navier-Stokes (RANS) equations. Finally section VIII. presents some conclusions, together with some future requirements for CFD.

II. Origins and goals of the JST scheme

The present author had actually embarked on a long term program since 1970 to develop computational fluid dynamics (CFD) for the purpose of airplane design. Starting with two dimensional transonic flow calculations for airfoils, the underlying strategy of this program was to make incremental advances in both the geometric complexity and the mathematical models of the flow, with the ultimate aim of calculating transonic and supersonic flows over complete aircraft, using at least the Euler equations of inviscid compressible flow as the mathematical model. The level of complexity that could be attempted at any stage of this program was paced by the available computing power, both processing speed and memory. In the early seventies, this was sufficient to calculate transonic potential flow solutions for airfoils, using, for example, *FLO 6*[10], but in the author's opinion not sufficient to attempt Euler solutions for any geometry of significant complexity. By 1975, it was feasible to calculate transonic potential flow solutions for swept wings using *FLO 22*[11], but the Control Data 6600, which represented the state of art in computing machinery, had only 131,000 words of core memory, with the consequence that the solution had to be stored on the disk, and computed plane by plane. *FLO 22* used an analytic transformation of the equations to a curvilinear coordinate system to represent the geometry. This approach could hardly be extended to any configuration more complex than an isolated wing. We overcame this difficulty in *FLO 27* by developing a discretization scheme for arbitrary body fitted hexahedral meshes[12]. Although we called this a finite volume scheme, it actually introduced isoparametric trilinear finite elements, stabilized by the addition of artificial diffusive terms to give an upwind bias. This method could have been used to calculate the flow over a complete aircraft if it was provided with a suitable mesh, but at that time the required mesh generation technology had yet to be developed. Ultimately, the French team from INRIA and Dassault[13] managed to calculate a transonic potential flow solution for a Falcon jet in 1982 using a finite element method on a tetrahedral mesh.

In the meanwhile, the present author had begun thinking seriously about ways to solve the Euler equations for steady flows, and first wrote an Euler solver, *EUL 1*[‡] in 1976, which integrated the time dependent equations to reach a steady state. This code used the Z scheme, defined as follows:

To solve the linear advection equation

$$\frac{\partial u}{\partial t} + a\frac{\partial u}{\partial x} = 0 \tag{1}$$

with $a > 0$ (a right running waver), the discrete scheme on a uniform mesh with time and space intervals Δt and Δx is

$$v_j^{n+1} = v_j^n - \frac{\lambda}{2}\left(v_j^{n+1} - v_{j-1}^{n+1}\right) - \frac{\lambda}{2}\left(v_{j+1}^n - v_j^n\right),$$

where v_j^n is the discrete solution at time level n and meshpoint j, and λ is the CFL number

$$\lambda = a\frac{\Delta t}{\Delta x}.$$

The scheme is semi-implicit with the illustrated stencil, similar to a single step version of the MacCormack scheme[14]. It is second order accurate and stable for an arbitrarily large positive CFL number λ. For a nonlinear problem such as

$$\frac{\partial u}{\partial t} + \frac{\partial}{\partial x}f(u) = 0,$$

[‡]The author still has a working copy of this code.

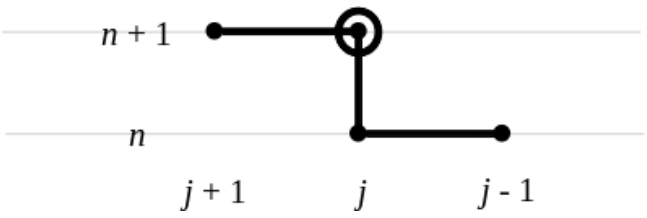

Figure 1: Z-scheme

the scheme takes the form

$$v_j^{n+1} = v_j^n - \frac{\Delta t}{2\Delta x}\left(f(v_j^{n+1}) - f(v_{j-1}^{n+1})\right) - \frac{\Delta t}{2\Delta x}\left(f(v_{j+1}^n) - f(v_j^n)\right),$$

which requires iterative solution for v_j^{n+1}. At locally supersonic points the difference scheme was switched to the second order accurate backward difference formula at both time levels n and $n+1$. This switch led to cleanly captured numerical shocks in transonic flow calculations. The resulting scheme reliably converged to a steady state and gave quite good results for simple geometries such as an axisymmetric boat tail. These studies of the Z-scheme were never published, and the scheme wound up being replaced by the LU implicit scheme[15] which could be regarded as forward and reverse sweeps of the Z-scheme to give unconditional stability for waves traveling in both directions.

In 1979 there was held a GAMM workshop in Stockholm on *"Numerical methods for the Computation of Inviscid Transonic Flow with Shock Waves"*, organized by Rizzi and Viviand. The results of a variety of methods to calculate both transonic potential flow and Euler solutions were presented and compared. The Euler methods generally relied on time marching, and it appeared that none of them could reach a steady state. This was the general state of affairs when the author was approached by Wolfgang Schmidt[§], then the leader of the CFD group at Dornier, with a proposal to visit Dornier for three weeks during the summer of 1980, and embark on a collaboration to produce an improved Euler solver.

Our primary goal from the outset was the calculation of fully converged steady state solutions, although since we were using a time marching method, we also envisaged dual use for both steady and unsteady flows. The starting point was an existing in-house code to solve the two dimensional Euler equations which had been written by Rizzi and Schmidt.[¶] This used a finite volume implementation of the MacCormack scheme[16]. Because the MacCormack scheme produces oscillations at shock waves, it was modified by the addition of artificial diffusive terms with a coefficient proportional to a sensor for sharp pressure gradients. In a one dimensional case, the form of the sensor is

$$\epsilon = \left|\frac{p_{j+1} - 2p_j + p_{j-1}}{p_{j+1} + 2p_j + p_{j-1}}\right| \leq 1,$$

where it is assumed that the pressure is positive. The code produced apparently reasonable answers but it would not fully converge to steady state. Moreover, the MacCormack scheme, like the Lax Wendroff scheme, bundles the space and time discretizations, with the consequence that a steady state solution, if it could be reached, would depend on the time step Δt. The first step in developing the new code was to replace the MacCormack scheme by a semi-discrete scheme which separated the space and time discretizations (also called the method of lines). At the same time, we concluded that we could use a simple central difference scheme for the spatial discretization and rely on added diffusive terms to prevent oscillations in the vicinity of shock waves. The time stepping scheme we first used was based on the idea of iterating the residuals of an implicit scheme. In order to solve

$$\frac{dw}{dt} + R(w) = 0,$$

where $R(w)$ is the space residual for the solution w, a second order accurate implicit scheme has the form

$$w^{n+1} = w^n - \frac{\Delta t}{2}\left(R(w^{n+1}) + R(w^n)\right).$$

[§]Sadly, Wolfgang Schmidt died of a sudden massive heart attack in 2008.

[¶]This code was extremely cleanly written and caused the author to completely revise his programming style to emphasize clarity.

At any time step, denoting $w^{(0)}$ as the starting value, a simple iterative procedure is to set

$$\begin{aligned} w^{(1)} &= w^{(0)} - \Delta t R(w^{(0)}) \\ w^{(2)} &= w^{(0)} - \frac{\Delta t}{2}\left(R(w^{(1)}) + R(w^{(0)})\right) \\ w^{(3)} &= w^{(0)} - \frac{\Delta t}{2}\left(R(w^{(2)}) + R(w^{(0)})\right) \\ \vdots &= \vdots \end{aligned}$$

It turns out from a linear analysis of the advection equation, that this iteration verges for CFL numbers ≤ 2, but there is no benefit in using more than 3 iterations, so we used a 3 stage scheme where $w^{(0)} = w^n$, $w^{n+1} = w^{(3)}$.

The second significant change we implemented was in the construction of the artificial diffusive terms. Because the finite volume equations are usually expressed as

$$V\frac{dw}{dt} + R(w) = 0,$$

where V is the cell area or volume, and $R(w)$ is the flux balance for the state vector, the existing Dornier code added diffusive terms which had the form

$$D_{i,j} = d_{i+\frac{1}{2},j} - d_{i-\frac{1}{2},j} + d_{i,j+\frac{1}{2}} - d_{i,j-\frac{1}{2}},$$

where the indices $i + \frac{1}{2}$ and $j + \frac{1}{2}$ denote the cell interfaces, while, for example, the diffusive flux for the density ρ had the form

$$d_{i+\frac{1}{2},j} = \epsilon((\rho V)_{i+1,j} - (\rho V)_{i,j}).$$

In the far field where ρ should eventually be constant, these diffusive terms reduce to differences of the cell areas or volumes, with the consequence that uniform flow would no longer satisfy the difference equations. In order to rectify this, it was essential to base the diffusive terms on differences of the state variables without including cell metrics. It remained necessary to determine an appropriate scaling. Since we wanted a steady state that would not depend on the time step Δt, we concluded that the scaling should depend on $\Delta t/\Delta t^*$, where Δt^* is the time step for a CFL number of unity, which may be estimated as follows. On a face with vector area $\boldsymbol{S}$ with magnitude $|S|$, denote the local velocity and speed of sound by $\boldsymbol{q}$ and c. Then define

$$qs = \boldsymbol{q} \cdot \boldsymbol{S}, \quad cs = c|S|.$$

Now in the case of a two dimensional flow

$$\Delta t^* = \frac{|S|}{(qs + cs)_i + (qs + cs)_j},$$

where $(qs + cs)_i$ and $(qs + cs)_j$ are average values of $qs + cs$ in each coordinate direction. The quantities $(qs + cs)_i$ and $(qs + cs)_j$ represent the spectral radii of the Jacobian matrices of the flux vectors in the i and j directions, so this scaling leads to diffusive terms scaled to the sum of the spectral radii, whereas it is now well known that it is sufficient to add diffusive terms scaled to the separate spectral radii in each coordinate direction. The use of the sum of the spectral radii, however, results in a scheme that is quite robust for grids containing high aspect ratio cells.

In order to accelerate convergence to a steady state, we used a variable local time step corresponding to a fixed CFL number, such that waves should propagate from the body to the far field in a fixed number of time steps proportional to the number of mesh intervals between the body and the far field. The code also provided for the inclusion of enthalpy damping to accelerate convergence to a steady state. An analysis of these ideas[15] suggests that it might be possible to obtain exponential convergence in time, while abandoning any aspiration to time accuracy for an unsteady flow calculation. A property of steady state Euler solutions is that the total enthalpy should be constant throughout the flow field. In order to satisfy this property, the diffusive terms for the energy equation were calculated from differences of the total enthalpy

instead of the total energy. It may be noted that subsequent characteristic based schemes, such as the Roe scheme[2], do not satisfy this property.

Initial tests at Dornier indicated that the new code produced significantly better results than the previous code. However, we remained unable to obtain fully converged steady state solutions. At this point, the author returned to America to take up a new faculty appointment at Princeton, and it was not until November that some new computational facilities (an IBM 4341 with a processing speed of about 0.15 MFLOPS and 2 MB memory) became available. After numerous tests, it was impossible to escape the conclusion that the scheme would not reliably converge to a steady state. Instead, the residuals would decrease by about three orders of magnitude in a few hundred steps, and then oscillate with a magnitude $\sim 10^{-3}$ and a period of around 50 steps.

At this point, it appeared that the failure to converge was due to wave reflections from the far field boundaries, and in consultation with Eli Turkel, we introduced far field boundary conditions based on linearized characteristics. However, this failed to solve the problem. Then, in a numerical experiment in which the artificial diffusion terms were scaled with a fixed coefficient instead of the pressure sensor, full convergence to a steady state was observed. This indicated that more dissipation was needed to guarantee convergence, but in this form the scheme would only be first order accurate. In order to achieve higher order accuracy, it would be necessary to use dissipative terms based on fourth differences rather than second differences, or correspondingly dissipative fluxes based on third differences.

The addition of third order dissipative fluxes indeed produced a convergent scheme, but it turned out that it also led to oscillations in the vicinity of shock waves, so it became apparent that these terms should be turned off if a shock wave could be detected. This led to the final form of the JST scheme as presented in the 1981 paper. A typical implementation for a one dimensional flow is as follows.

Denoting the density, pressure, velocity and energy by ρ, p, u and E, the governing equations are

$$\frac{\partial w}{\partial t} + \frac{\partial}{\partial x} f(w) = 0,$$

where the state and flux vectors are

$$w = \begin{bmatrix} \rho \\ \rho u \\ \rho E \end{bmatrix}, \quad f = \begin{bmatrix} \rho u \\ \rho u^2 + p \\ \rho u H \end{bmatrix}$$

and

$$p = (\gamma - 1)\rho \left(E - \frac{u^2}{2} \right), \quad H = E + \frac{p}{\rho}.$$

On a uniform grid with mesh interval Δx, the semi-discrete finite volume scheme takes the form

$$\Delta x \frac{dw_j}{dt} + h_{j+\frac{1}{2}} - h_{j-\frac{1}{2}} = 0,$$

where w_j denotes the average state in cell j, and $h_{j+\frac{1}{2}}$ denotes the numerical flux across the interface between cells j and $j+1$. In the JST scheme, the numerical flux is evaluated as

$$h_{j+\frac{1}{2}} = \frac{1}{2}(f_{j+1} + f_j) - d_{j+\frac{1}{2}},$$

where $f_j = f(w_j)$. The dissipative flux is

$$d_{j+\frac{1}{2}} = \epsilon^{(2)}_{j+\frac{1}{2}} \Delta w_{j+\frac{1}{2}} - \epsilon^{(4)}_{j+\frac{1}{2}} \left(\Delta w_{j+\frac{3}{2}} - 2\Delta w_{j+\frac{1}{2}} + \Delta w_{j-\frac{1}{2}} \right),$$

where

$$\Delta w_{j+\frac{1}{2}} = \begin{bmatrix} \rho_{j+1} - \rho_j \\ (\rho u)_{j+1} - (\rho u)_j \\ (\rho u H)_{j+1} - (\rho u H)_j \end{bmatrix}.$$

The spectral radius of the Jacobian matrix $\frac{\partial f}{\partial w}$ in cell j is $r_j = |u| + c$, where c is the local speed of sound. The dissipative coefficients $\epsilon^{(2)}_{j+\frac{1}{2}}$ and $\epsilon^{(4)}_{j+\frac{1}{2}}$ are switched on and off by a pressure sensor

$$s_j = \left| \frac{p_{j+1} - 2p_j + p_{j-1}}{p_{j+1} + 2p_j + p_{j-1}} \right|.$$

Interface values of the spectral radius and sensor may be defined as

$$r_{j+\frac{1}{2}} = \max(r_{j+1}, r_j), \quad s_{j+\frac{1}{2}} = \max(s_{j+1}, s_j).$$

Then,

$$\epsilon^{(2)}_{j+\frac{1}{2}} = \kappa_2 s_{j+\frac{1}{2}} r_{j+\frac{1}{2}}$$

and

$$\epsilon^{(4)}_{j+\frac{1}{2}} = \max(0, \kappa_4 r_{j+\frac{1}{2}} - c_4 \epsilon^{(2)}_{j+\frac{1}{2}}),$$

where for a transonic flow calculation, typical values of the constants are

$$\kappa_2 = 1, \quad \kappa_4 = \frac{1}{32}, \quad c_4 = 2.$$

In any case, κ_2 should be chosen to give enough lower order dissipation to prevent oscillations in the vicinity of shock waves, while c_4 should be large enough to make sure that the higher order terms are turned off when the lower order dissipation is active.

It should be noted that in a smooth region of the flow, both dissipative terms scale as $\mathcal{O}(\Delta x^3)$, because the sensor scales as $\mathcal{O}(\Delta x^2)$ and accordingly $\epsilon^{(2)}_{j+\frac{1}{2}}$ scales as $\mathcal{O}(\Delta x^2)$ and $\epsilon^{(4)}_{j+\frac{1}{2}}$ scales as $\mathcal{O}(1)$, while $\Delta w_{j+\frac{1}{2}}$ scales as $\mathcal{O}(\Delta x)$ and the third differences scale as $\mathcal{O}(\Delta x^3)$. For this reason, quite accurate results can be obtained without resorting to characteristic based fluxes. In fact, the numerical flux with the scalar diffusive coefficient $\epsilon^{(2)}_{j+\frac{1}{2}}$ is essentially equivalent to the Rusanov flux [17], with enthalpy differences substituted for energy differences in the energy flux.

Numerous variations of the scheme can be devised, and many have been tested over the years. For example, the convective flux can be evaluated as $f_{cj+\frac{1}{2}} = f(\bar{w})$, where $\bar{w} = \frac{1}{2}(w_{j+1} + w_j)$. Fairly recently, the author showed that if one first forms the averages

$$\bar{\rho} = \frac{1}{2}(\rho_{j+1} + \rho_j), \quad \bar{u} = \frac{1}{2}(u_{j+1} + u_j), \quad \bar{H} = \frac{1}{2}(H_{j+1} + H_j),$$

and constructs the convective flux as

$$f_{cj+\frac{1}{2}} = \begin{bmatrix} \bar{\rho} \\ \bar{\rho}\bar{u} \\ \bar{\rho}\bar{u}\bar{H} \end{bmatrix},$$

the basic discrete scheme without added dissipation satisfies a discrete kinetic energy conservation law.

Alternative switching functions can also easily be devised. A sharper sensor is

$$\frac{\left| \Delta p_{j+\frac{1}{2}} - \Delta p_{j-\frac{1}{2}} \right|}{\max\left(\left(\left| \Delta p_{j+\frac{1}{2}} \right| + \left| \Delta p_{j-\frac{1}{2}} \right| \right), p_{\lim} \right)},$$

where $\Delta p_{j+\frac{1}{2}} = p_{j+1} - p_j$ and $p_{\lim}$ is a small tolerance to ensure that s_j is defined when p is constant. With this definition $s_j = 1$ when p_j is an extremum, so that $p_{j+1} - p_j$ and $p_j - p_{j-1}$ have opposite signs, but now s_j scales as $\mathcal{O}(\Delta x)$ in a smooth region of the flow. This sensor has proved effective in shock tube simulations. It has also been found that it is sometimes beneficial to use a switch which sense variations in the density or the entropy. It is shown in section V. that

with the right choice of a switching function, the JST scheme is actually a total variation diminishing scheme for a scalar conservation law.

At this stage, we also re-examined the time stepping scheme. After conversations with Eli Turkel, we realized that it might be possible to improve on the three stage scheme. Actually this belongs to the class of Runge-Kutta schemes, and the stability region of the classical fourth order Runge-Kutta scheme indicates that one should be able to use a CFL number of $2\sqrt{2}$ with the four stage scheme compared with 2 for the three stage scheme, and this ought to be slightly more efficient. In order to solve a set of equations of the form

$$\frac{dw}{dt} + R(w) = 0,$$

the classical fourth order Runge-Kutta scheme is

$$\begin{aligned} w^{(1)} &= w^{(0)} - \frac{1}{2}\Delta t R(w^{(0)}), \\ w^{(2)} &= w^{(0)} - \frac{1}{2}\Delta t R(w^{(1)}), \\ w^{(3)} &= w^{(0)} - \Delta t R(w^{(2)}), \\ w^{(4)} &= w^{(0)} - \frac{1}{6}\Delta t \left(R(w^{(0)}) + 2R(w^{(1)}) + 2R(w^{(2)}) + R(w^{(3)}) \right), \end{aligned} \tag{2}$$

where $w^{(0)} = w^n$ and $w^{(4)} = w^{n+1}$. This scheme is fourth order accurate for nonlinear problems. But if one is only concerned about the steady state, it can be replaced by the following scheme which is fourth order accurate for linear problems, and has reduced memory requirements:

$$\begin{aligned} w^{(1)} &= w^{(0)} - \frac{\Delta t}{4} R(w^{(0)}), \\ w^{(2)} &= w^{(0)} - \frac{\Delta t}{3} R(w^{(1)}), \\ w^{(3)} &= w^{(0)} - \frac{\Delta t}{2} R(w^{(2)}), \\ w^{(4)} &= w^{(0)} - \Delta t R(w^{(3)}). \end{aligned}$$

This eliminates the need to store the intermediate solutions.

For steady state calculations, a further reduction in the computational costs can be achieved as follows. Suppose the residual $R(w)$ is split into a convective part $Q(w)$ and a dissipative part $D(w)$, arising from the artificial dissipation. In the case of Navier-Stokes simulations, this would also include the true viscous terms. Then the idea is to freeze the dissipative terms after the first stage.

$$\begin{aligned} w^{(1)} &= w^{(0)} - \frac{\Delta t}{4} \left(Q(w^{(0)}) + D(w^{(0)}) \right), \\ w^{(2)} &= w^{(0)} - \frac{\Delta t}{3} \left(Q(w^{(1)}) + D(w^{(0)}) \right), \\ w^{(3)} &= w^{(0)} - \frac{\Delta t}{2} \left(Q(w^{(2)}) + D(w^{(0)}) \right), \\ w^{(4)} &= w^{(0)} - \Delta t \left(Q(w^{(3)}) + D(w^{(0)}) \right). \end{aligned} \tag{3}$$

This substantially reduces the computational cost, while it turns out that the stability region of the modified scheme is about the same size as the standard fourth order Runge-Kutta scheme. This scheme actually does not belong to the class of standard Runge-Kutta schemes, but rather to the class of additive Runge-Kutta schemes in which different terms of the equations are not treated in the same way. Schemes of this type have only relatively recently been the subject of mathematical analysis [18,19].

The overall formulation of the JST scheme was actually guided by a number of design principles as listed below:

(1) The scheme should be in conservation form to ensure satisfaction of the shock jump conditions, according to the theorem of Lax and Wendroff.

(2) Second order accuracy in smooth regions of the flow.

(3) Shock waves should be captured without overshoots or oscillations, at least in the steady state (but overshoots during the transient phase would be tolerated).

(4) The steady state should be independent of the time evolution.

(5) The scheme should be stable when using variable local time steps at a fixed CFL number, to accelerate convergence to a steady state.

(6) The discrete steady state solution should have constant stagnation enthalpy, consistent with properties of the true steady state solutions.

These principles dictated several aspects of the scheme. In particular, in order to satisfy principle (4), the time integration scheme should be separated from the space discretization scheme by first constructing a semi-discrete approximation. This rules out the Lax-Wendroff and MacCormack schemes for which the steady state solution depends on the time step Δt in the case of two- or three-dimensional problems. This issue is particularly important when variable local time steps are used in steady state calculations. When the mesh is stretched to a large distance from the body, the far field cells may become very large, with correspondingly large values of Δt.

In practice, the new scheme consistently converged to non-oscillatory steady state solutions of transonic flows with shock waves over airfoils. Accordingly the author programmed to the scheme for three-dimensional flows over swept wings in February 1981. The IBM 4341 computer which we had installed in the MAE Department at Princeton was not adequate for three dimensional calculations, but Cray Research agreed to run the code on their in-house machines. Eventually this code, *FLO 57*, was used worldwide by the aerospace industry. It was the precursor of codes such as the Lockheed TEAM code and the NASA code TLNS3D. Cray Research supplied *FLO 57* to the British RAE and the Dutch NLR bundled with the sale of Cray computers. In England, it was developed into a multi-block solver by the Aircraft Research Association, and was also the basis of the EJ30 code at British Aerospace. As an example of the industrial use of *FLO 57* and its derivatives figure 2 shows a comparison between the predicted and measured drag rise of the Northrup YF-23. This calculation, which was performed by R. J. Busch Jr.[20], actually preceded the wind tunnel tests.

III. Convergence acceleration: residual averaging and multigrid

After getting *FLO 57* to work, the author's immediate focus was to further accelerate convergence to a steady state. The first significant advance was the introduction of residual averaging[21]. In this approach, the permissible time step is increased by replacing the residual at each point by a weighted average of residuals at neighboring points. If we consider multi-stage schemes of the type described in the previous section, in the one dimensional case, one might replace the residual R_j by the average

$$\bar{R}_j = \epsilon R_{j-1} + (1-2\epsilon)R_j + \epsilon R_{j+1} \tag{4}$$

at each stage of the scheme. This smooths the residuals and also increases the support of the scheme, thus relaxing the restriction on the time step imposed by the Courant-Friedrichs-Lewy condition. As long as $\epsilon < \frac{1}{4}$, the absolute value $|A|$ decreases with increasing wave numbers ξ in the range $0 \le \xi \le \pi$. If $\epsilon = \frac{1}{4}$, however, $\bar{R}_j = 0$ for the odd-even mode $R_j = (-1)^j$.

In order to avoid a restriction on the smoothing coefficient, it is better to perform the averaging implicitly by setting

$$-\epsilon\bar{R}_{j-1} + (1-2\epsilon)\bar{R}_j - \epsilon\bar{R}_{j+1} = R_j. \tag{5}$$

This corresponds to a discretization of the inverse Helmholtz operator. For an infinite interval, this equation has the explicit solution

$$\bar{R}_j = \frac{1-r}{1+r}\sum_{q=-\infty}^{\infty} r^{|q|}R_{j+q}, \tag{6}$$

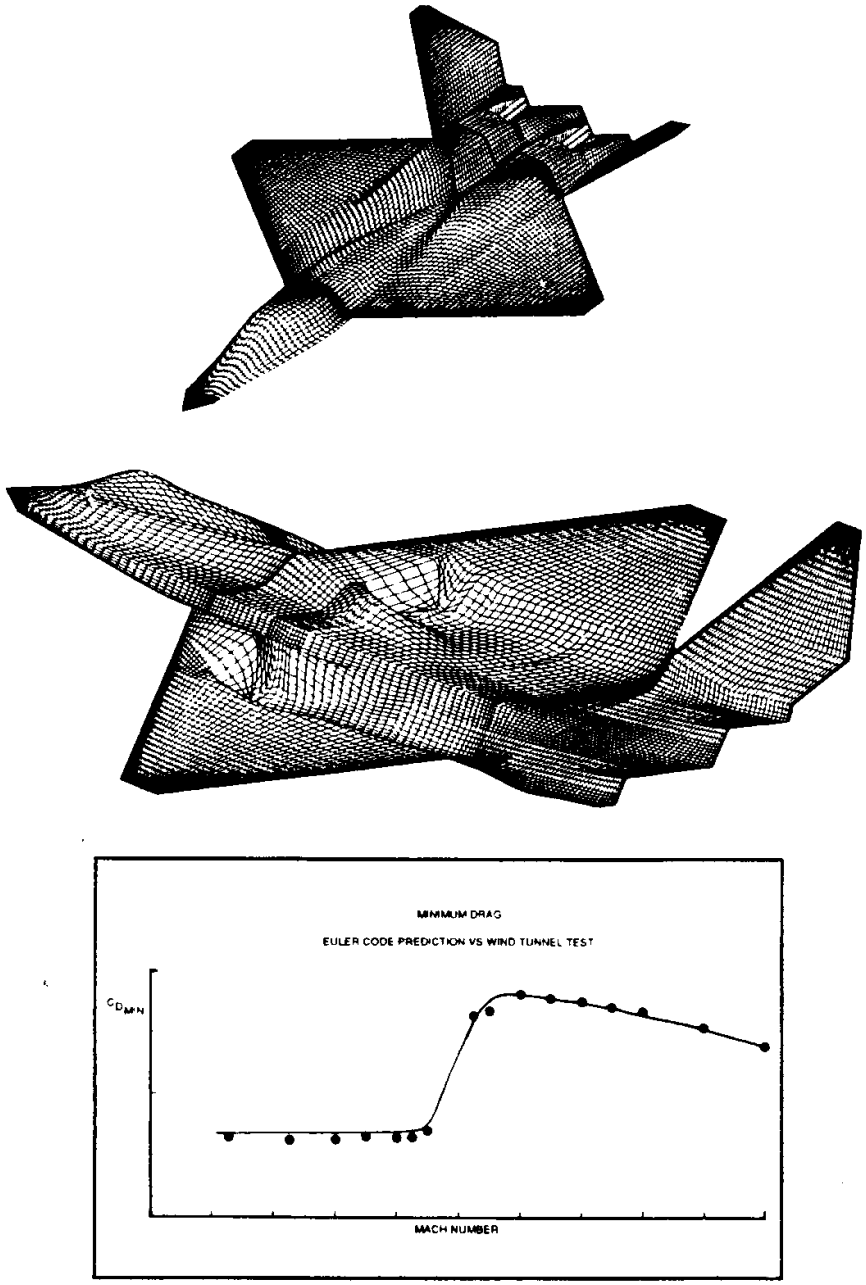

Figure 2: Comparison of experimental and computed drag rise curve for the YF-23 (Supplied by R. J. Bussh Jr.).

where

$$\epsilon = \frac{r}{(1-r)^2}, \quad r < 1.$$

It may be determined by Fourier analysis that in the case of linear advection, we can perform stable calculations at any desired CFL number λ by using a large enough smoothing coefficient such that

$$\epsilon \geq \frac{1}{4}\left(\left(\frac{\lambda}{\lambda^*}\right)^2 - 1\right),$$

where λ^* is the stability limit of the original time stepping scheme.

The second and more decisive step was the incorporation of a multigrid time stepping scheme. The author actually formulated and coded this scheme in the spring of 1981, and had hoped to include some results in the 1981 paper. Unfortunately, the initial numerical experiments with the scheme failed to show any acceleration. Meanwhile, Ni presented a multigrid Euler solver based on an adaptation of the Lax-Wendroff scheme[22]. During 1982, the author resumed efforts to get the Runge-Kutta multigrid (RKMG) scheme to work, and found some alternative time stepping schemes with good high frequency damping properties. At first the scheme still failed, but finally it turned out that the source of the failure was a mistake in the main program in which two of the multigrid subroutines were called in the wrong order. Otherwise, the code might have worked in 1981.

Although the term agglomeration multigrid is generally associated with unstructured meshes, it appears that the RKMG scheme was the first to use an agglomeration procedure. Successively coarser grids were formed by agglomerating four cells on the finer grid to form a single coarse grid cell. A summary of the scheme is given in the following paragraphs.

Consider a sequence of successively coarser quadrilateral grids generated by deleting alternate points in each coordinate direction as illustrated in figure 3. The mesh cells at each coarser level roughly correspond to cells formed by agglomerating groups of 4 cells from the finer level, although they do not exactly coincide if the mesh is curved. In order to give a precise description of the multigrid scheme, we use subscripts to indicate the grid level, with the finest grid denoted as level 1. The simplest multigrid cycle is a "sawtooth" cycle of the type illustrated in figure 4, in which the solution is updated by the time stepping scheme at each grid level on the way down to the coarsest level, and then the corrections are successively interpolated to the next finer level on the way up to the finest grid, without any additional updates by the time-stepping scheme. The solution at level 1 is updated by the basic m-stage scheme

$$\begin{aligned} w_1^{(1)} &= w_1^{(0)} - \alpha_1 \Delta t R_1^{(0)} \\ &\vdots \quad\quad \vdots \\ w_1^{(q)} &= w_1^{(0)} - \alpha_q \Delta t R_1^{(q-1)} \\ &\vdots \quad\quad \vdots \\ w_1^{(m)} &= w_1^{(0)} - \Delta t R_1^{(m-1)}, \end{aligned} \tag{7}$$

where $w_1^{(0)}$ is the value at the beginning of the time step and $w_1^{(m)}$ is the final value at the end of the step, while the residual at any stage is calculated by the additive RK scheme.

To complete the description of the multigrid scheme, several transfer operations need to be defined. First, the solution vector on grid k must be initialized as

$$w_k^{(0)} = Q_{k,k-1} w_{k-1}, \tag{8}$$

where w_{k-1} is the current value on grid $k-1$, and $Q_{k,k-1}$ is a transfer operator. Next, it is necessary to calculate a residual forcing function such that the solution on grid k is driven by the residuals calculated on grid $k-1$. This can be accomplished by setting

$$P_k = T_{k,k-1} R_{k-1}(w_{k-1}) - R_k\left(w_k^{(0)}\right), \tag{9}$$

where $T_{k,k-1}$ is a residual transfer operator which aggregates the residuals from grid $k-1$. Note these residuals should be re-evaluated, using the final values w_{k-1} after the completion of the updating process on grid $k-1$. Now on grid k,

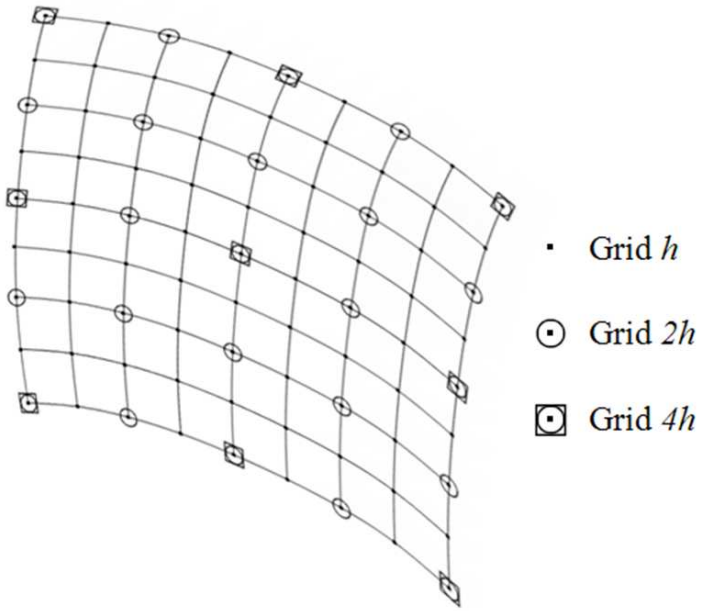

Figure 3: Nested grids with 3 levels for a multigrid scheme.

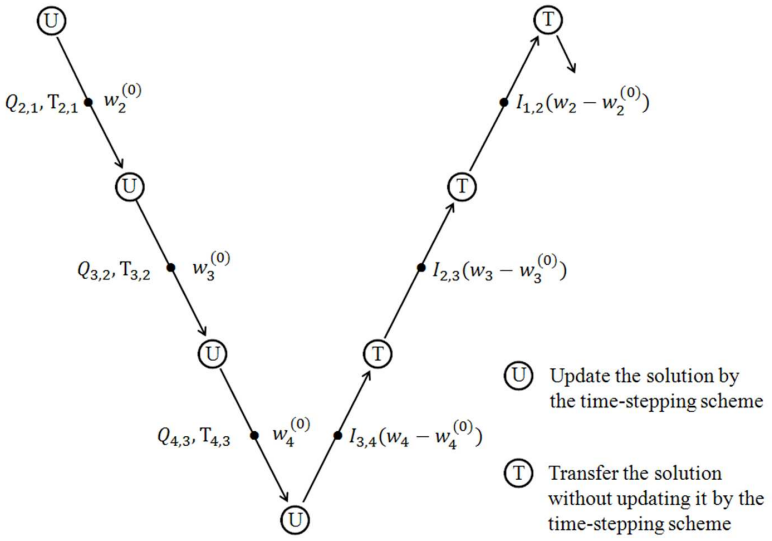

Figure 4: Sawtooth multigrid cycle.

we replace the residual $R_k(w_k)$ by $R_k(w_k) + P_k$ at each stage of the time-stepping scheme. Thus, the multistage scheme is reformulated as

$$\begin{aligned} w_k^{(1)} &= w_k^{(0)} - \alpha_1 \Delta t_k \left(R_k^{(0)} + P_k \right) \\ &\vdots \quad\quad \vdots \\ w_k^{(q)} &= w_k^{(0)} - \alpha_q \Delta t_k \left(R_k^{(q-1)} + P_k \right) \\ &\vdots \quad\quad \vdots \\ w_k^{(m)} &= w_k^{(0)} - \Delta t_k \left(R_k^{(m-1)} + P_k \right). \end{aligned}$$

The result $w_k^{(m)}$ provides the initial data for grid $k+1$. Finally, during the ascent back up the levels to the finest grid, the accumulated change $w_k - w_k^{(0)}$ is transferred to grid $k-1$ with the aid of an interpolation operator $I_{k-1,k}$.

It should be noted that at any grid level below the finest mesh, the residual calculated in the first stage is $R_k^{(0)} = R_k \left(w_k^{(0)} \right)$, and this is canceled by the second term in P_k, with the result that the first stage update is determined purely by the aggregated residuals from grid $k-1$. If these are zero, $w_k^{(1)} = w_k^{(0)}$, and it follows that no change is made to the solution at any of the later stages. Thus, if the values of the solution on the finest grid satisfy the equations exactly, they will be left unchanged by the entire multigrid cycle. This is an essential requirement for a successful multigrid scheme.

For a sequence of nested grids of the type illustrated in figure 3, the solution and residual transfer operators $Q_{k,k-1}$ and $T_{k,k-1}$ may be chosen as follows. The values of the flow variables are transferred to the next coarser grid by the rule

$$w_{k,m}^{(0)} = \frac{\sum\limits_n S_n w_{k-1,n}}{\sum\limits_n S_n},$$

where the sum is over the 4 cells on grid $k-1$, which are agglomerated to correspond to cell m on grid k, and S_n is the area of cell n on grid $k-1$. This rule conserves mass, momentum and energy. The residual transfer operator is simply

defined by summing the residuals of the cells on grid $k-1$ which correspond to cell m on grid k, so at cell m, on grid k

$$P_{k,m} = r \sum_n R_{k-1,n} - R_{k,m} \left(w_k^{(0)} \right),$$

where r is a relaxation factor which is normally set equal to unity. In more difficult cases, however, such as hypersonic flow, or extremely stretched meshes, it is sometimes useful to reduce r to values in the range 0.5 to 0.75. The factor r is also useful for debugging, because we can set r to zero to simulate the case when the solution on grid k satisfies the equations exactly, and produces zero residuals. In that case, none of the coarser grid levels should change the solution, and its evolution should be identical to the evolution of the solution with a single fine grid. This helps to identify possible conflicts between the coarse levels and the fine level, that may be introduced, for example, by boundary conditions on the coarse levels which are incompatible with the fine grid boundary conditions.

In order to transfer the corrections from grid k to grid $k-1$, we may use bilinear interpolation between the centers of the 4 coarse grid cells which contain the center of a particular fine grid cell. On a nonuniform curvilinear grid, this would require different interpolation formulas at every grid point. In practice, good results have been obtained by assuming that the mesh could be mapped to a Cartesian mesh in which each coarse mesh cell exactly corresponds to 4 fine mesh cells. The interpolation operator may then be based on bilinear interpolation on the corresponding Cartesian mesh, as illustrated in figure 5. Accordingly, with the notation of the figure,

$$\begin{aligned}
\Delta w_{f1} &= \frac{9}{16}\Delta w_{c1} + \frac{3}{16}\Delta w_{c2} + \frac{3}{16}\Delta w_{c3} + \frac{1}{16}\Delta w_{c4} \\
\Delta w_{f2} &= \frac{9}{16}\Delta w_{c2} + \frac{3}{16}\Delta w_{c1} + \frac{3}{16}\Delta w_{c4} + \frac{1}{16}\Delta w_{c3} \\
\Delta w_{f3} &= \frac{9}{16}\Delta w_{c3} + \frac{3}{16}\Delta w_{c1} + \frac{3}{16}\Delta w_{c4} + \frac{1}{16}\Delta w_{c2} \\
\Delta w_{f4} &= \frac{9}{16}\Delta w_{c4} + \frac{3}{16}\Delta w_{c2} + \frac{3}{16}\Delta w_{c3} + \frac{1}{16}\Delta w_{c1},
\end{aligned}$$

where Δw_{f1}, Δw_{f2}, Δw_{f3} and Δw_{f4} denote the corrections in cells f_1, f_2, f_3 and f_4 on grid $k+1$, and Δw_{c1}, Δw_{c2}, Δw_{c3} and Δw_{c4} denote the accumulated change $w_k - w_k^{(0)}$ in the solution vector in cells c_1, c_2, c_3 and c_4 of grid k. This change is the total change affected by operators on all the coarser grids.

If the time step Δt_k is doubled at each coarser level, a 5-level sawtooth cycle could ideally advance the solution by an accumulated interval

$$\Delta t + 2\Delta t + 4\Delta t + 8\Delta t + 16\Delta t = 31\Delta t,$$

where Δt is the time step on the fine mesh. At the same time, the computational cost of the updates by the time-stepping scheme scales as

$$1 + \frac{1}{4} + \frac{1}{8} + \frac{1}{16} + \frac{1}{32} + \cdots < \frac{4}{3}$$

in a two dimensional calculation, or

$$1 + \frac{1}{8} + \frac{1}{64} + \frac{1}{512} + \frac{1}{4096} + \cdots < \frac{8}{7}$$

in a three dimensional calculation, to which there must be added a relatively small overhead due to the transfer operations.

In practice, the repeated interpolation operations generate high frequency errors on each higher level grid, and these need to be damped by the time-stepping scheme. Accordingly, the time stepping scheme should be designed to behave like a low pass filter with the maximum possible attenuation of the high frequency modes with wave numbers in the band $\frac{\pi}{2} \le \xi \le \pi$.

While the sawtooth cycle is quite effective, it has been found that W-cycles of the type illustrated in figure 7 provide additional acceleration. Once the 3-level W-cycle has been defined, W-cycles with more levels may be generated recursively as shown in the figure. In a W-cycle, the solution is updated twice on level 2, four times on level 3, and so on until

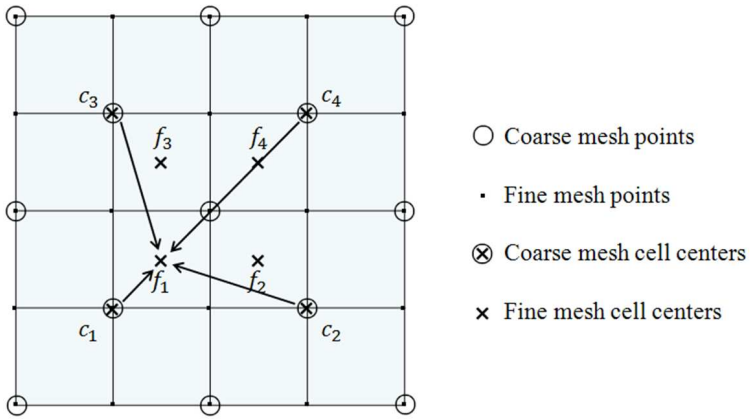

Figure 5: Interpolation scheme.

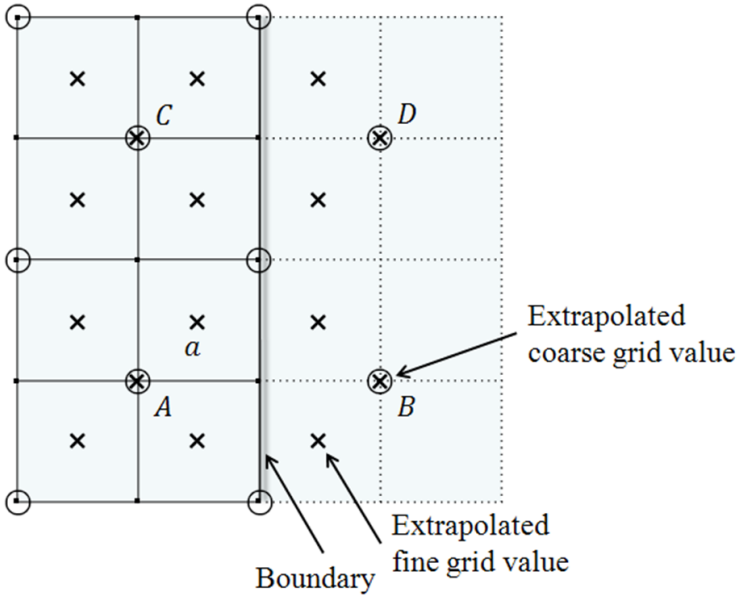

Figure 6: Influence of extrapolated boundary values: Corrections to the interior fine grid point a depend on an extrapolated coarse grid values at B and D.

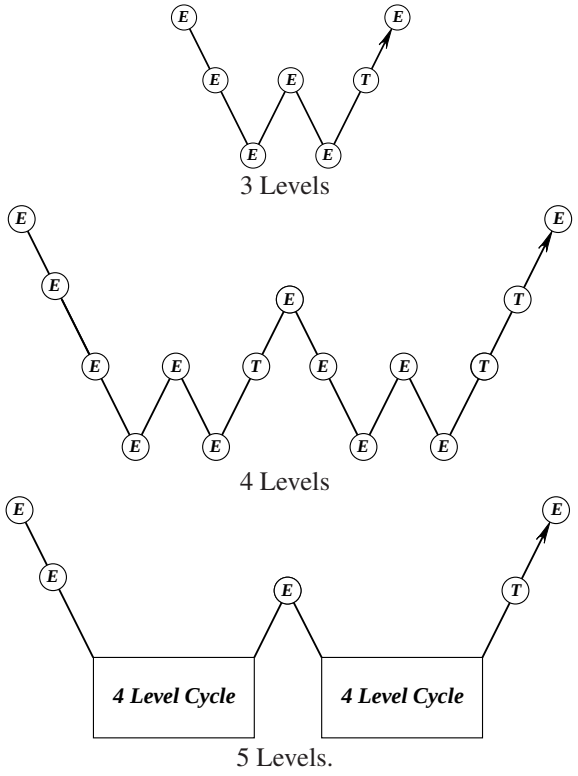

Figure 7: Multigrid W-cycle for managing the grid calculation. E, evaluate the change in the flow for one step; T, transfer the data without updating the solution.

the coarsest level is reached, where the number of updates is the same as the number on the second last level. Thus, if Δt_k is doubled at each coarser level, the effective time interval for a 4-level W-cycle is

$$\Delta t + 4\Delta t + 16\Delta t + 64\Delta t = 85\Delta t,$$

while the computational cost of the updates by the time-stepping scheme scales as

$$1 + \frac{2}{8} + \frac{4}{64} + \frac{4}{512} < \frac{4}{3}$$

for a three dimensional calculation.

The actual speed up realized in practice will be less than this because of the imperfections in the transfer operations, but it can still be very large. It should be noted, moreover, that multigrid methods simultaneously drive the solution towards equilibrium at all the grid levels. Consequently, global quantities such as the lift coefficient converge at the same rate as the local residuals, whereas on a single grid, the local residuals may be very small, while the global solution is still far from equilibrium.

The performance of the multigrid scheme can be further enhanced by the use of specially designed time stepping schemes. The following class of additive Runge-Kutta schemes[23] has proven to be particularly effective. Suppose that the residual is split into convective and diffusive parts as

$$R(w) = Q(w) + D(w),$$

where $Q(w)$ is the convective part and $D(w)$ is the dissipative or diffusive part. With this split, the schemes have the form

$$\begin{aligned} w^{(1)} &= w^{(0)} - \alpha_1 \Delta t \left(Q^{(1)} + D^{(1)} \right), \\ &\vdots \qquad \vdots \\ w^{(k)} &= w^{(0)} - \alpha_k \Delta t \left(Q^{(k-1)} + D^{(k-1)} \right), \end{aligned} \tag{10}$$

where $\alpha_m = 1$, and

$$Q^{(0)} = Q\left(w^{(0)}\right), \quad D^{(0)} = D\left(w^{(0)}\right), \tag{11}$$

and

$$\begin{aligned} Q^{(k)} &= Q\left(w^{(k)}\right), \\ D^{(k)} &= \beta_k D\left(w^{(k)}\right) + (1-\beta_k) D^{(k-1)}. \end{aligned} \tag{12}$$

The coefficients α_k are chosen to maximize the stability interval along the imaginary axis, while the coefficients β_k are chosen to increase the stability interval along the negative real axis.

Two schemes which have been found to be particularly effective are tabulated below. The first is a four-stage scheme with two evaluations of dissipation (4-2 scheme). Its coefficients are

$$\begin{aligned} \alpha_1 &= \tfrac{1}{3}, & \beta_1 &= 1, \\ \alpha_2 &= \tfrac{4}{15}, & \beta_2 &= \tfrac{1}{2}, \\ \alpha_3 &= \tfrac{5}{9}, & \beta_3 &= 0, \\ \alpha_4 &= 1, & \beta_4 &= 0. \end{aligned} \tag{13}$$

The second is a five-stage scheme with three evaluations of dissipation (5-3 scheme). Its coefficients are

$$\begin{aligned} \alpha_1 &= \tfrac{1}{4}, & \beta_1 &= 1, \\ \alpha_2 &= \tfrac{1}{6}, & \beta_2 &= 0, \\ \alpha_3 &= \tfrac{3}{8}, & \beta_3 &= 0.56, \\ \alpha_4 &= \tfrac{1}{2}, & \beta_4 &= 0, \\ \alpha_5 &= 1, & \beta_5 &= 0.44. \end{aligned} \tag{14}$$

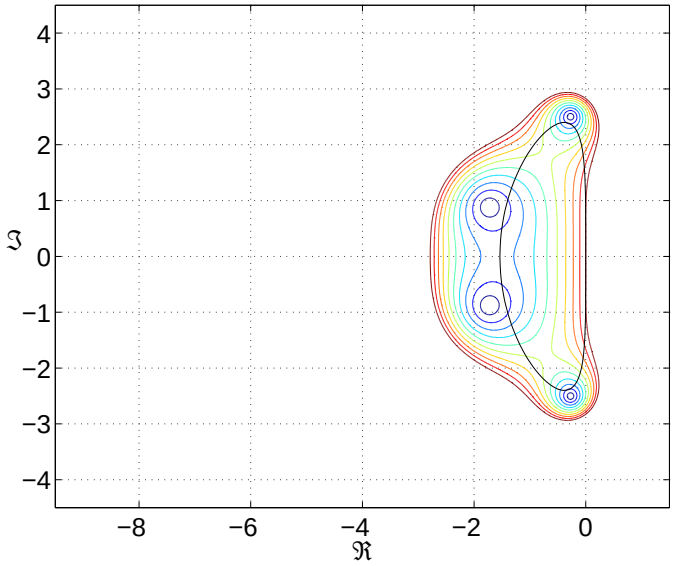

Figure 8: Stability region for the standard 4-stage RK scheme (equation (2)). Black line '—' is the locus of Fourier symbol for linear advection with CFL number 2.4.

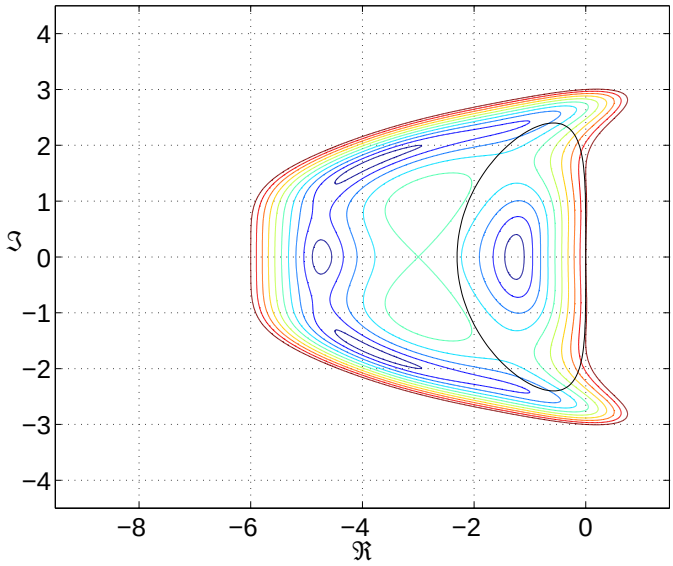

Figure 9: Stability region for the 4-2 scheme (equation (13)). Black line '—' is the locus of Fourier symbol for linear advection with CFL number 2.4.

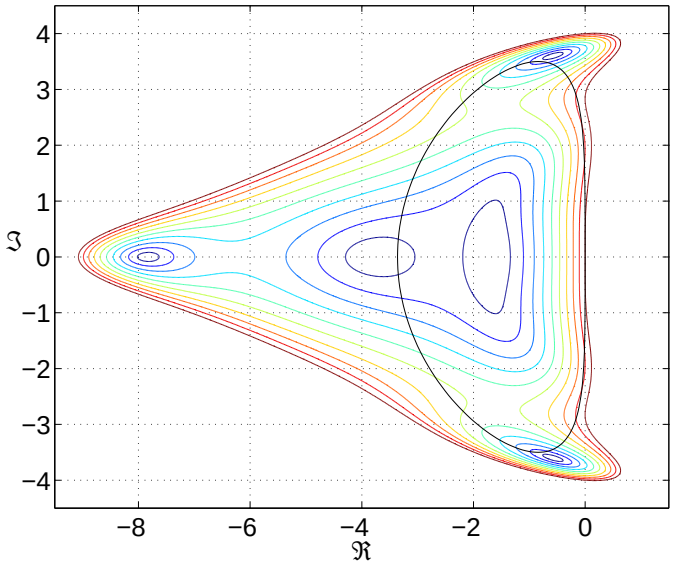

Figure 10: Stability region for the 5-3 scheme (equation (14)). Black line '—' is the locus of Fourier symbol for linear advection with CFL number 3.5.

Figures 8, 9 and 10 display the stability regions for the standard fourth order RK4 scheme (2) and the 4-2 and 5-3 schemes defined by equations (13 and 14). The expansion of the stability region is apparent. They also show the locus of the Fourier symbol using the linear advection equation as a representative model problem[24], with third order artificial diffusion in an amount chosen to damp high frequency modes.

Figure 11 shows the result of a multigrid calculation of the same benchmark test case that has been used in the previous sections, transonic flow past an NACA 0012 airfoil at Mach 0.8 and an angle of attack of 1.25 degrees, discretized by the JST scheme. This calculation used a 5-level W cycle with the 5-3 additive Runge-Kutta scheme defined by equation (13). The solution is well converged after 50 cycles. Moreover, it can be seen from the second curve in figure 11b that the lift coefficient reaches a steady state in about 25 cycles. Figure 12 shows the same calculation repeated with $\epsilon^{(2)}$ set equal to zero. There is now a large oscillation ahead of the shock wave on the upper surface. The rate of convergence to a steady state, however, is almost exactly the same. If, on the other hand, $\epsilon^{(4)}$ is set to zero, the calculation does not converge. This highlights the separate roles of $\epsilon^{(2)}$ and $\epsilon^{(4)}$. The first coefficient is needed purely to enable non-oscillatory capture of shock waves, while the second is needed purely to ensure convergence to a steady state.

IV. Unstructured meshes

The other major direction in the evolution of the JST scheme was the extension to unstructured meshes, in joint work with Tim Baker[‖] and Nigel Weatherill. Alternative approaches to the treatment of complex configurations such as a complete aircraft include the use of Cartesian meshes with special formulas for immersed boundaries or cut boundary cells, or multiblock and overset body fitted structured meshes. The author believed that it would be very difficult to extend Cartesian mesh methods to the Reynolds averaged Navier-Stokes (RANS) equations. On the other hand, developing the mesh generation technology for body fitted structured meshes would be a major undertaking. Thus it seemed that the quickest route to calculating the flow about a complete aircraft would be to use a body fitted tetrahedral mesh.

During 1984, the author experimented with both vertex and cell centered schemes for Euler solutions on triangular meshes. Both schemes gave satisfactory results. In the case of a three dimensional tetrahedral mesh, however, there are

[‖] Sadly, Tim Baker died prematurely with pancreatic cancer in 2006.

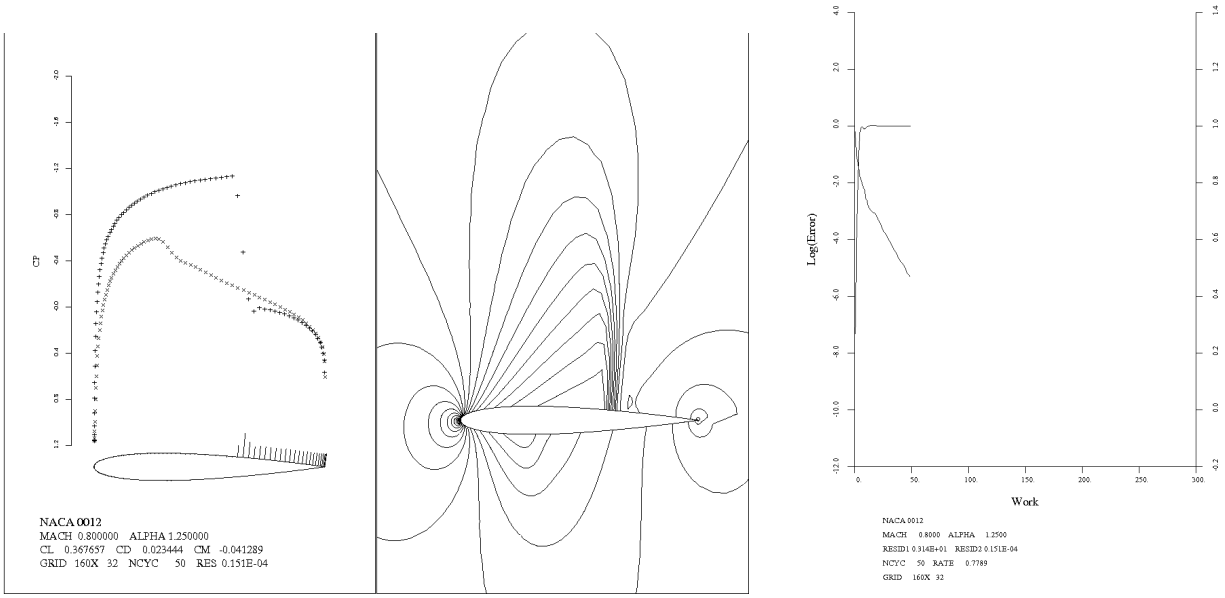

(a) (b)

Figure 11: NACA 0012. Steady state flow solution using multigrid acceleration method.

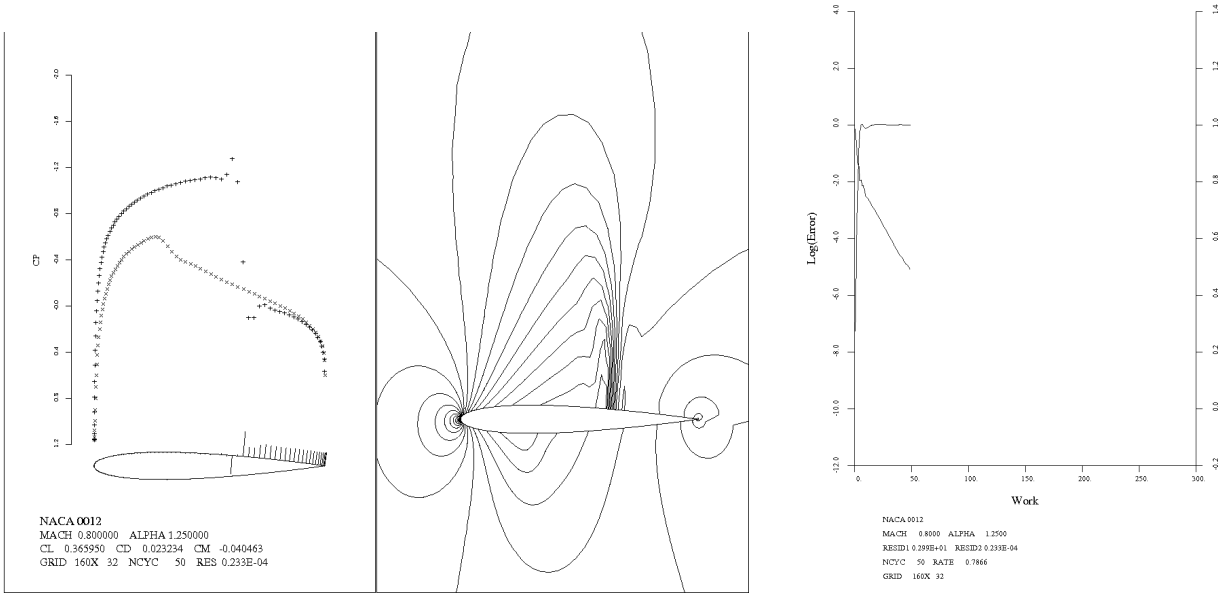

(a) (b)

Figure 12: NACA 0012. Steady state flow solution using multigrid acceleration method and setting $\epsilon^{(2)} = 0$.

typically about six times as many cells as there are nodes, and it appeared that a vertex centered formulation would be more feasible, given the memory limitations of the available computers at that time.

Tim baker had joined Princeton as a Senior Research Scientist in 1982. Early in 1985, Nigel Weatherill arrived in Princeton a six month sabbatical leave from the Aircraft Research Association, and we agreed that he should investigate the Delaunay triangulation method for mesh generation. After some successful experiments with two dimensional configurations, we decided to attempt a calculation of a complete commercial aircraft within the year. The author focused on writing a new flow solver, while Tim Baker and Nigel Weatherill tackled the problems of mesh generation, which proved to be harder than we had originally anticipated. Nigel Weatherill had to return to England before we had succeeded in generating a proper mesh, and it fell on Tim Baker to complete the work. Cray Research supported us by providing access to an in-house Cray 1. However, because our code used the entire memory of the machine, we only had access during overnight sessions at weekends, and we had to go there because the only way to visualize the mesh was to use the Evans and Sutherland graphics terminals while Cray had installed. We finally got a mesh for a Boeing 747 with flow through nacelles in late November, and were able to present our first results at the AIAA Aerospace Sciences Meeting in Reno in January 1986[25].

The vertex centered discretization scheme can be derived directly from the integral form of the gas dynamics equations, in the case of a two dimensional flow

$$\frac{d}{dt}\int_{\mathcal{D}} w dS + \oint_{\mathcal{B}} (f(w)\, dy - g(w)\, dx) \tag{15}$$

for a domain $\mathcal{D}$ with boundary $\mathcal{B}$. Denoting the density, pressure, velocity components and energy as before by p, ρ, u, v and E, the state and flux vectors are

$$w = \begin{bmatrix} \rho \\ \rho u \\ \rho v \\ \rho E \end{bmatrix}, \quad f = \begin{bmatrix} \rho u \\ \rho u^2 + p \\ \rho uv \\ \rho uH \end{bmatrix}, \quad g = \begin{bmatrix} \rho v \\ \rho vu \\ \rho v^2 + p \\ \rho vH \end{bmatrix},$$

where

$$p = (\gamma - 1)\rho\left(E - \frac{u^2 + v^2}{2}\right), \quad H = E + \frac{p}{\rho}.$$

The discrete scheme for the convective terms is as follows.

Suppose that a particular interior node, labeled 0 for convenience, as illustrated in figure 13, is surrounded by n nearest neighbors $k = 1, \ldots, n$, where node $n + 1$ is identified with node 1, which also form n surrounding cells. The area of the control volume is

$$S_0 = \sum_{k=1}^{n} S_k,$$

where S_k is the area of cell k.

Then, using trapezoidal integration, we approximate the integral form (15) as

$$S_0 \frac{df_0}{dt} + \frac{1}{2}\sum_{k=1}^{n} ((f_{k+1} + f_k)(y_{k+1} - y_k) - (g_{k+1} + g_k)(x_{k+1} - x_k)) = 0, \tag{16}$$

where

$$f_k = f(w_k), \quad g_k = g(w_k).$$

It was shown in the 1986 paper that these equations are equivalent to the equations which result from a Galerkin finite element method with linear elements, subject to a scaling factor of 3, provided that the mass matrix is lumped. As it stands the scheme is not suitable for capturing shock waves in transonic or supersonic flow, and it needs to be stabilized by the addition of upwind biasing terms. For this purpose, it can be rearranged as an edge based scheme in the following manner.

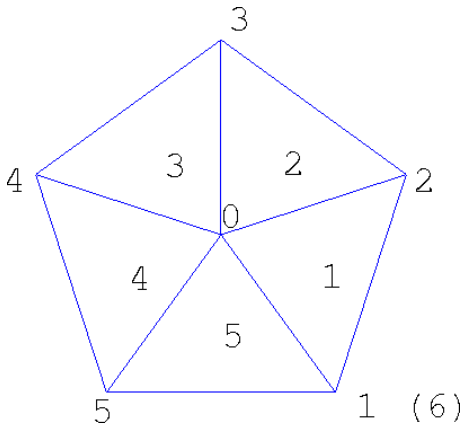

Figure 13: Cells and nodes surrounding the vertex 0.

Since f_k and g_k contribute to the flux across the edges from $k-1$ to k and k to $k+1$ in the trapezoidal integration rule, they actually make a contribution

$$\frac{1}{2}(f_k(y_{k+1}-y_{k-1})-g_k(x_{k+1}-x_{k-1})).$$

Associating the intervals

$$\Delta y_{k0}=y_{k+1}-y_{k-1},\quad \Delta x_{k0}=x_{k+1}-x_{k-1},$$

with the edge $k0$, equation (16) is thus equivalent to

$$S_0\frac{dw_0}{dt}+\frac{1}{2}\sum_{k=1}^{n}(f_k\Delta y_{k0}-g_k\Delta x_{k0})=0.$$

However, since the sums of Δy_{k0} and Δx_{k0} are zero around a closed loop, we can add or subtract f_0 and g_0 to obtain the equivalent radial edge based schemes

$$S_0\frac{dw_0}{dt}+\frac{1}{2}\sum_{k=1}^{n}((f_k+f_0)\Delta y_{k0}-(g_k+g_0)\Delta x_{k0})=0, \tag{17}$$

and

$$S_0\frac{dw_0}{dt}+\frac{1}{2}\sum_{k=1}^{n}((f_k-f_0)\Delta y_{k0}-(g_k-g_0)\Delta x_{k0})=0. \tag{18}$$

It is then possible to add stabilizing diffusive terms along each edge. To construct a characteristic based scheme using the Roe flux, for example, we define a generalized Roe matrix A_{k0} along the edge $k0$ satisfying

$$A_{k0}(w_k-w_0)=(f_k-f_0)\Delta y_{k0}-(g_k-g_0)\Delta x_{k0}.$$

Then we subtract an artificial diffusion term $\frac{1}{2}|A_{k0}|(w_k-w_0)$ along each edge to produce the upwind scheme

$$S_0\frac{dw_0}{dt}+\frac{1}{2}\sum_{k=1}^{n}((f_k+f_0)\Delta y_{k0}-(g_k+g_0)\Delta x_{k0}-|A_{k0}|(w_k-w_0))=0, \tag{19}$$

which may equivalently be written as

$$S_0\frac{dw_0}{dt}=\frac{1}{2}\sum_{k=1}^{n}(|A_{k0}|-A_{k0})(w_k-w_0).$$

We can also formulate a scheme with scalar diffusion

$$S_0 \frac{dw_0}{dt} + \frac{1}{2}\sum_{k=1}^{n}((f_k + f_0)\Delta y_{k0} + (g_k - g_0)\Delta x_{k0} - \epsilon_{k0}(w_k - w_0)) = 0, \tag{20}$$

where

$$\epsilon_{k0} = \max|\lambda(A_{k0})|.$$

The schemes (19) and (20) are only first order accurate. In the case of the scheme (20) with scalar diffusion, a relatively simple way to obtain a more accurate scheme is to recycle the edge differencing procedure [25]. The accumulated dissipative term in equation (20) from all the edges may be written as

$$D_0^{(1)} = \sum_{k=1}^{n} \epsilon_{k0}^{(1)}(w_k - w_0), \tag{21}$$

where now the superscript 1 is included to denote that this is the first order dissipative term. In order to define a higher order dissipative term, we set

$$E_0 = \sum_{k=1}^{n}(w_k - w_0) \tag{22}$$

at every mesh point, and then set

$$D_0^{(2)} = \sum_{k=1}^{n} \epsilon_{k0}^{(2)}(E_k - E_0). \tag{23}$$

The Jameson-Schmidt-Turkel (JST) scheme can now be emulated by blending $D_0^{(1)}$ and $D_0^{(2)}$ and adapting the coefficients $\epsilon_{k0}^{(1)}$ and $\epsilon_{k0}^{(2)}$ to the local pressure gradient. This was the scheme that was used to calculate the flow past a Boeing 747 in December 1985. It has proved to be robust, and it has been found to have good shock capturing capabilities. Figures 16 and 17 show the original calculation for the Boeing 747. Figures 18-20 show some representative calculations on finer meshes using the same code, while we called the Airplane code.

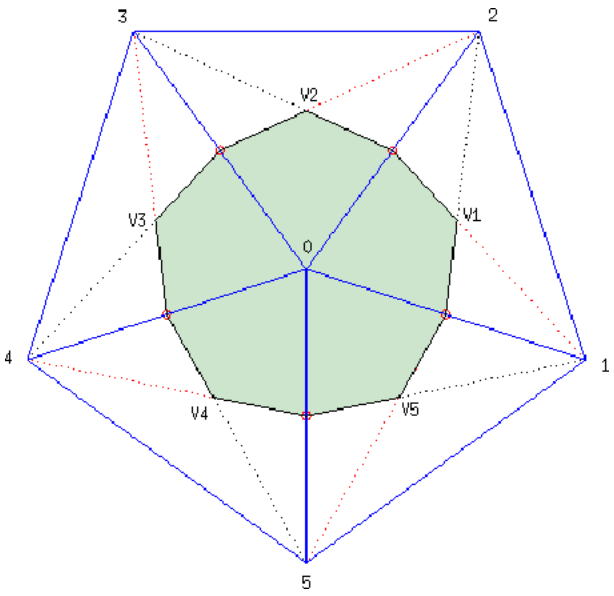

Figure 14

In recent years, finite volume schemes based on median dual meshes have become quite popular. Such a scheme was apparently first proposed by Vijayasundaram[26]. Moreover, it is easy to show that at interior points, the scheme presented in this section is in fact exactly equivalent to a finite volume scheme using median dual control volumes. Referring to figure 14, the median dual control volume is defined by connecting the centroids V_k of each neighboring cell to the midpoints of the edges $k0$. Since 1/3 of the area of each neighboring cell is assigned to the median dual control volume, its area is equal to $\frac{1}{3}\sum_{k=1}^{n} S_k$. Now, the flux along edge $k0$ is calculated as

$$\frac{1}{2}((f_k + f_0)(y(V_k) - y(V_{k-1})) - (g_k + g_0)(x(V_k) - x(V_{k-1}))).$$

Due to the construction from the medians, however,

$$y(V_k) - y(V_{k-1}) = \frac{1}{3}\Delta y_{k0},$$

$$x(V_k) - x(V_{k-1}) = \frac{1}{3}\Delta x_{k0}.$$

Thus, the formulas are exactly equivalent to equation (17) multiplied by 1/3. Since the median dual control volumes exactly cover the domain without overlapping, it is immediately evident that the scheme is conservative.

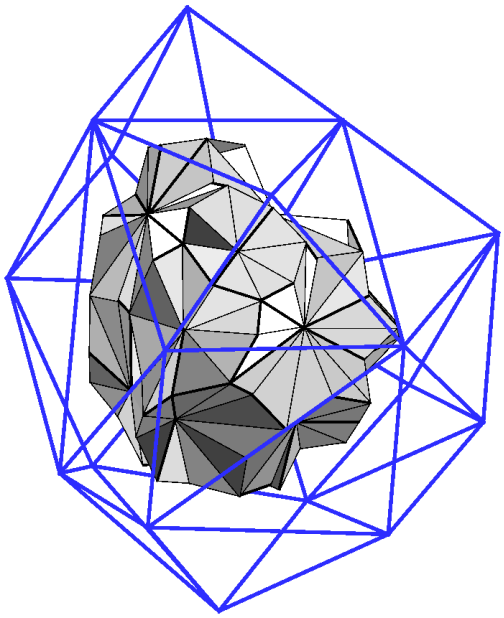

Figure 15: Aggregated and median dual control volumes.

The equivalence of schemes using aggregated and dual control volumes can also be proven in the three dimensional case[27], with a scaling factor of 4, although there is little apparent similarity between the control volumes, as illustrated in figure 15.

V. Reformulation of the JST scheme as a total variation diminishing (TVD) scheme

Harten's introduction of the concept of total variation diminishing (TVD) schemes offered a rational approach to the construction of non-oscillatory shock capturing schemes, and provoked a general rethinking of CFD algorithms for

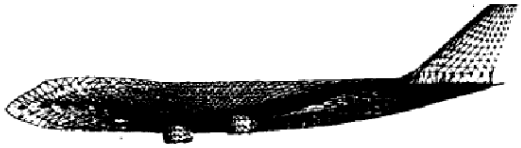

Figure 16: Surface mesh distribution for the Boeing 747-200.

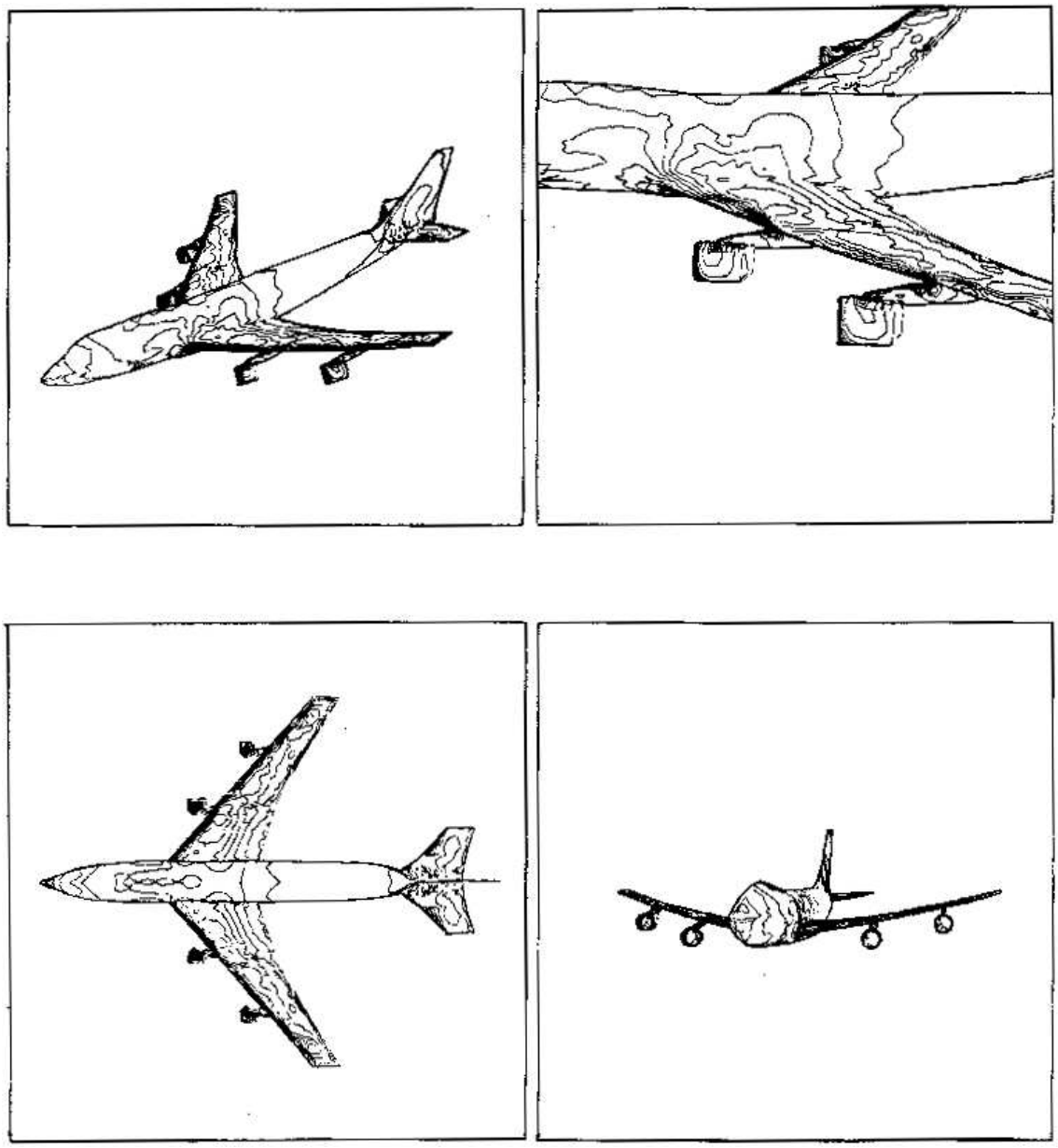

Figure 17: Pressure contours on the aircraft surface; $M = 0.84$, $\alpha = 2.73°$.

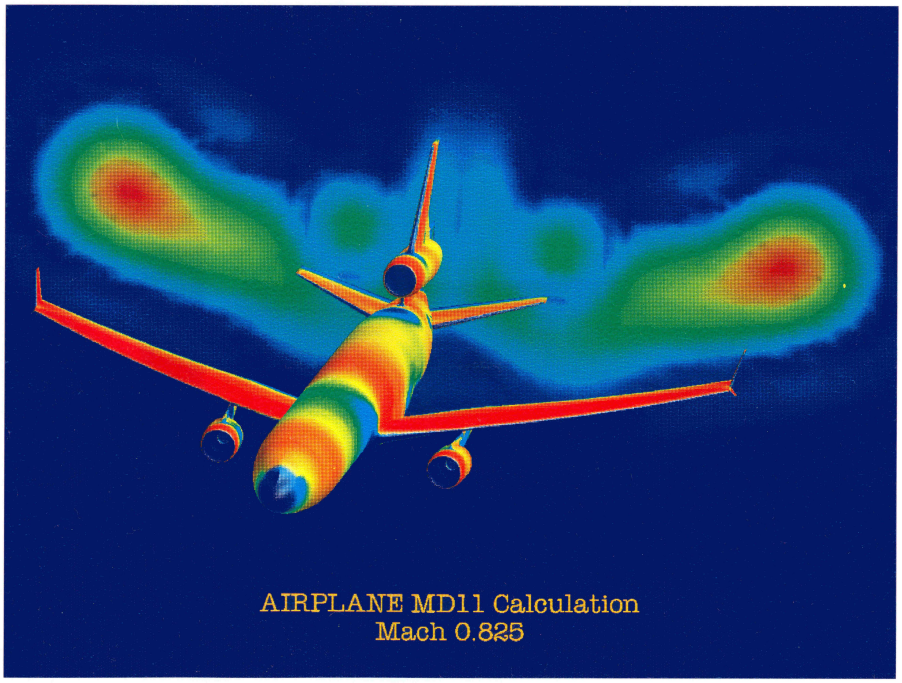

Figure 18: Pressure distribution over MD11, $Ma = 0.825$.

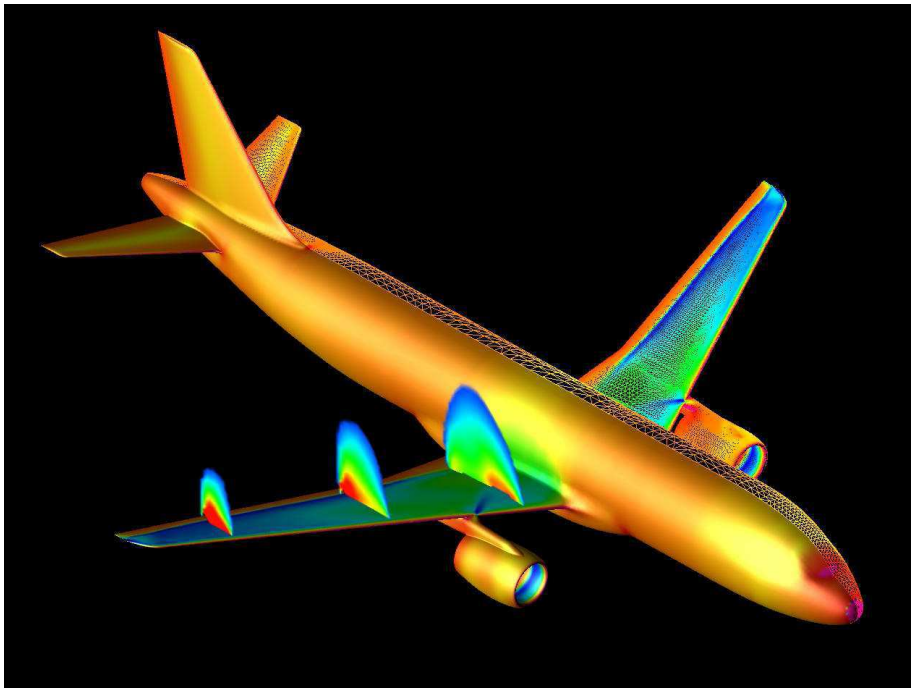

Figure 19: Contours of Mach number over A320 wing surface.

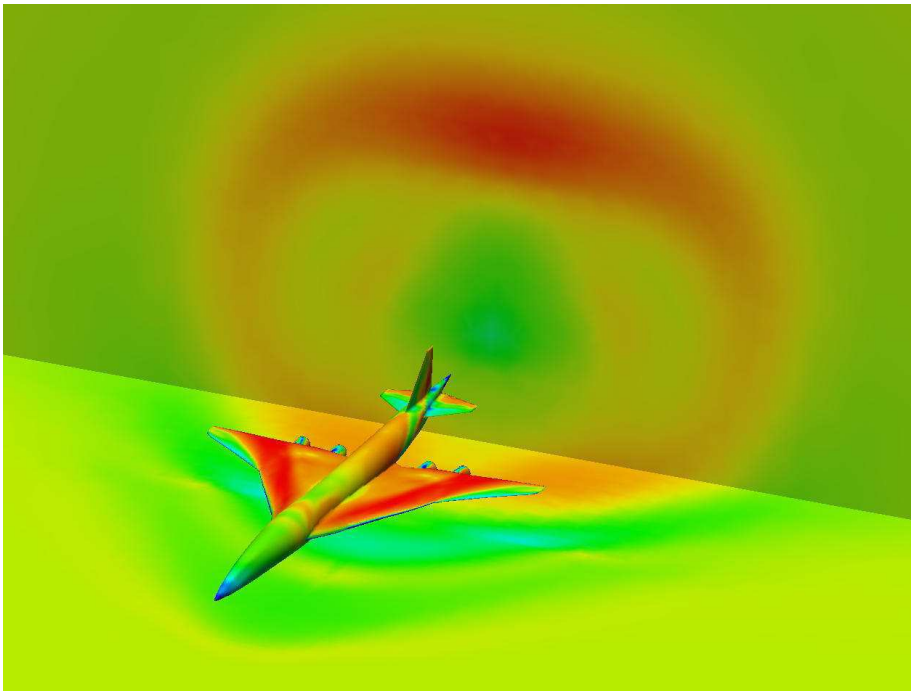

Figure 20: Pressure distribution over NASA High Speed Civil Transport, $Ma = 2.4$.

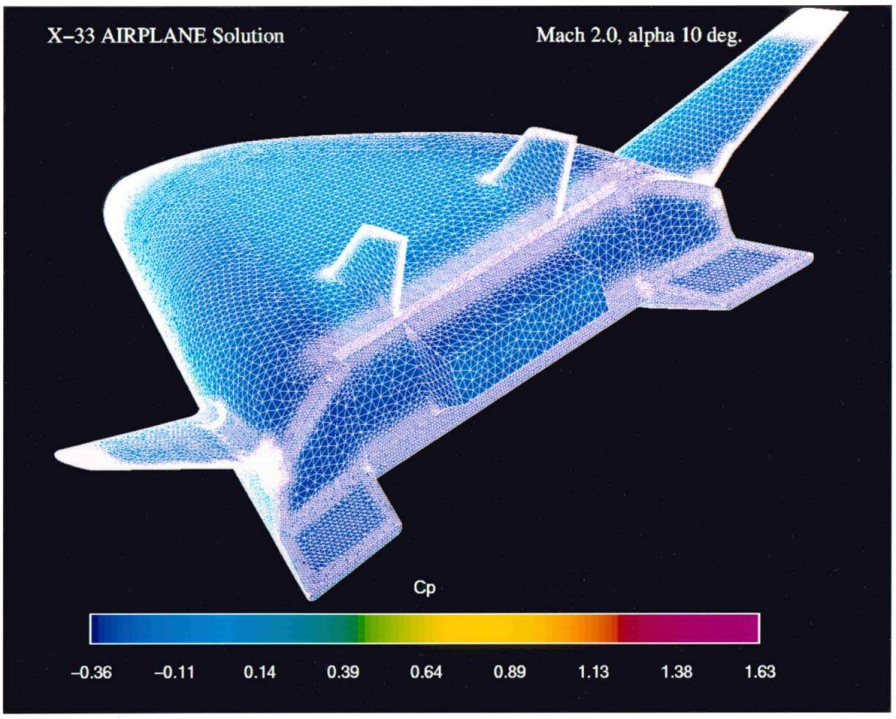

Figure 21: Pressure distribution over X33, $Ma = 2.0$.

compressible flow. Harten's theory applies to scalar conservation laws, but it provides a useful guideline to the treatment of systems of conservation laws, such as the gas dynamics equations. It is the purpose of this section to show that when applied to a scalar conservation law, the JST scheme can readily be reformulated as a TVD scheme. The TVD concept is appealing because the total variation, defined as

$$TV(u) = \int_a^b \left| \frac{\partial u}{\partial x} \right| dx$$

for a function u, or

$$TV(v) = \sum_{j=1}^{n} |v_{j+1} - v_j|$$

for a discrete sequence v_j, is a direct measure of oscillation.

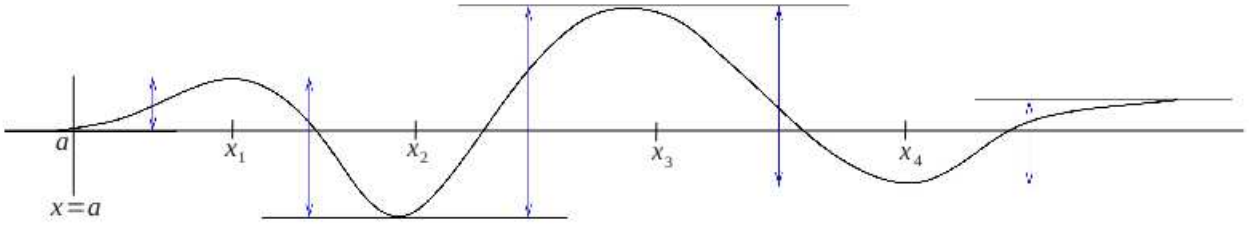

Figure 22: Equivalent LED and TVD schemes (one dimensional case)

It is useful to note, however, that the total variation is closely related to the local extrema of a function or sequence. Referring to figure (22), it can be seen each extremum contributes to the total variation for the segments on either side up to the next extrema. Let x_j, $j = 1, 2, ..., n-1$, be the interior extrema of $u(x)$, and augment these with the endpoints $x_0 = a$ and $x_n = b$. It can be seen that over an interval in which $u(x)$ is increasing, say x_{j-1} to x_j, the contribution to $TV(u)$ is $u(x_j) - u(x_{j-1})$, while over the following interval in which $u(x)$ is decreasing the contribution to $TV(u)$ is $u(x_j) - u(x_{j+1})$. Thus

$$\begin{aligned} TV(u) &= 2\sum(\text{interior maxima}) \\ &\quad -2\sum(\text{interior minima}) \\ &\quad \pm(\text{the end values}). \end{aligned} \tag{24}$$

Similarly in the discrete case

$$\begin{aligned} TV(v) &= 2\sum(\text{interior maxima}) \\ &\quad -2\sum(\text{interior minima}) \\ &\quad \pm v_0 \pm v_n. \end{aligned} \tag{25}$$

It follows that a local extremum diminishing (LED) scheme, constructed such that local extrema cannot increase, is also a TVD scheme. It is also the case that local extrema do not increase in true solutions of non-linear conservation laws, because these solutions remain constant along characteristics, and shock waves do not produce new extrema. It is easy to state the conditions for an LED scheme, and moreover, these conditions also hold for multi-dimensional problems on both structured and unstructured meshes.

Consider the general discrete scheme

$$v_i^{n+1} = \sum_j c_{ij} v_j^n,$$

where the solution at time level $n+1$ depends on the solution over an arbitrarily large stencil of points at time level n. If this approximates an equation with no source term, and v_j is constant at time level n, then the solution should remain unchanged. Accordingly for consistency,

$$\sum_j c_{ij} = 1.$$

But

$$\left|v_i^{n+1}\right| \le \sum_j |c_{ij}| \left|v_j^n\right| \le \left(\sum_j |c_{ij}|\right) \max_j \left|v_j^n\right|.$$

Thus $\left|v_i^{n+1}\right|$ will be bounded by the extrema in the stencil if

$$\sum_j |c_{ij}| \le 1.$$

This is only possible if

$$c_{ij} \ge 0.$$

Moreover, local extrema cannot increase if the stencil is compact, with $c_{ij} = 0$ and if the mesh points i and j are not nearest neighbors.

A general semi-discrete scheme has the form

$$\frac{dv_i}{dt} = \sum_j a_{ij} v_j.$$

If this approximates an equation with no source term, $\frac{dv_i}{dt} = 0$ if v_j is constant and accordingly for consistency,

$$\sum_j a_{ij} = 0.$$

It follows that the semi-discrete scheme can be rewritten as

$$\frac{dv_i}{dt} = \sum_{j \ne i} a_{ij}(v_j - v_i)$$

without loss of generality. Now, if the coefficients

$$a_{ij} \ge 0, \quad j \ne i,$$

it follows that

$$\frac{dv_i}{dt} \le 0 \text{ if } v_i \text{ is a local maximum}$$

and

$$\frac{dv_i}{dt} \ge 0 \text{ if } v_i \text{ is a local minimum.}$$

Thus, the scheme will be LED if it has a compact stencil with positive coefficients.

It is easy to see that any semi-discrete LED scheme can be converted into a corresponding fully discrete forward Euler LED scheme

$$\begin{aligned} v_i^{n+1} &= v_i^n + \Delta t \sum_{j \ne i} a_{ij} \left(v_j^n - v_i^n\right) \\ &= \left(1 - \Delta t \sum_{j \ne i} a_{ij}\right) v_i^n + \sum_{j \ne i} \Delta t \, a_{ij} v_j^n, \end{aligned}$$

where now the diagonal coefficient will be non-negative if the time step satisfies the generalized CFL condition

$$\left(\sum_{j\neq i}^{i} a_{ij}\right)\Delta t \leq 1.$$

Dating back to the work of Godunov[8], it has been known that schemes that are guaranteed to produce monotonic solutions through shock waves can be at most first order accurate. This was the dilemma, highlighted by Van Leer in his sequence of papers[3–7], which must be addressed in any attempt to develop higher order schemes, generally labeled "high resolution schemes" in the decade 1980 - 1990. In order to develop a higher order scheme which is LED and consequently TVD, the first step, however, is to construct 3-point first order accurate schemes. One route to this is to introduce artificial diffusive terms which produce an upwind bias. Suppose that the scalar conservation law

$$\frac{\partial u}{\partial t} + \frac{\partial}{\partial x} f(u) = 0$$

is approximated by the semi-discrete scheme

$$\Delta x \frac{dv_j}{dt} + h_{j+\frac{1}{2}} - h_{j-\frac{1}{2}} = 0$$

where v_j represents the average value of u in cell j, and $h_{j+\frac{1}{2}}$ is the numerical flux across the interface separating cells j and $j+1$. Introducing artificial diffusion, we define the numerical fluxes

$$h_{j+\frac{1}{2}} = \frac{1}{2}(f_{j+1} + f_j) - \alpha_{j+\frac{1}{2}}(v_{j+1} - v_j)$$

where

$$f_j = f(v_j)$$

and $\alpha_{j+\frac{1}{2}}$ is the coefficient of artificial diffusion. Define also a numerical estimate of the wave speed $a(u) = f'(u)$ as

$$a_{j+\frac{1}{2}} = \begin{cases} \dfrac{f_{j+1} - f_j}{v_{j+1} - v_j}, & v_{j+1} \neq v_j \\ \left.\dfrac{\partial f}{\partial u}\right|_{v_j}, & v_{j+1} = v_j \end{cases} \tag{26}$$

Now the numerical fluxes can be expressed as

$$h_{j+\frac{1}{2}} = f_j + \frac{1}{2}\left(f_{j+1} - f_j\right) - \alpha_{j+\frac{1}{2}}\left(v_{j+1} - v_j\right) = f_j - \left(\alpha_{j+\frac{1}{2}} - \frac{1}{2}a_{j+\frac{1}{2}}\right)\left(v_{j+1} - v_j\right)$$

and

$$h_{j-\frac{1}{2}} = f_j - \frac{1}{2}\left(f_j - f_{j-1}\right) - \alpha_{j-\frac{1}{2}}(v_j - v_{j-1}\Big) = f_j - \left(\alpha_{j-\frac{1}{2}} + \frac{1}{2}a_{j-\frac{1}{2}}\right)\left(v_j - v_{j-1}\right)$$

Thus the semi-discrete scheme reduces to

$$\Delta x \frac{dv_j}{dt} = \left(\alpha_{j+\frac{1}{2}} - \frac{1}{2}a_{j+\frac{1}{2}}\right)\left(v_{j+1} - v_j\right) + \left(\alpha_{j-\frac{1}{2}} + \frac{1}{2}a_{j-\frac{1}{2}}\right)\left(v_{j-1} - v_j\right)$$

Accordingly it is LED if for all j

$$\alpha_{j+\frac{1}{2}} \geq \frac{1}{2}\left|a_{j+\frac{1}{2}}\right|.$$

The least diffusive LED scheme is obtained by setting

$$\alpha_{j+\frac{1}{2}} = \frac{1}{2}|a_{j+\frac{1}{2}}|$$

to produce the diffusive flux

$$d_{j+\frac{1}{2}} = \frac{1}{2}|a_{j+\frac{1}{2}}|\Delta v_{j+\frac{1}{2}}$$

where

$$v_{j+\frac{1}{2}} = v_{j+1} - v_j$$

This is the pure first order upwind scheme, since if $a_{j+\frac{1}{2}} > 0$

$$d_{j+\frac{1}{2}} = \frac{1}{2}\frac{f_{j+1} - f_j}{v_{j+1} - v_j}(v_{j+1} - v_j) = \frac{1}{2}(f_{j+1} - f_j)$$

and if $a_{j+\frac{1}{2}} < 0$,

$$d_{j+\frac{1}{2}} = -\frac{1}{2}(f_{j-1} - f_j).$$

Thus,

$$h_{j+\frac{1}{2}} = \begin{cases} f_j & \text{if} \quad a_{j+\frac{1}{2}} > 0 \\ \frac{1}{2}(f_{j+1} + f_j) & \text{if} \quad a_{j+\frac{1}{2}} = 0 \\ f_{j+1} & \text{if} \quad a_{j+\frac{1}{2}} < 0 \end{cases} \tag{27}$$

Thus, the upwind scheme is the least diffusive first order accurate LED scheme.

It is now relatively straightforward to reformulate the JST scheme as an LED/TVD scheme. In the JST scheme, the numerical flux is

$$h_{j+\frac{1}{2}} = \frac{1}{2}(f_{j+1} + f_j) - d_{j+\frac{1}{2}}, \tag{28}$$

where the diffusive flux has the form

$$d_{j+\frac{1}{2}} = \epsilon^{(2)}_{j+\frac{1}{2}}\Delta v_{j+\frac{1}{2}} - \epsilon^{(4)}_{j+\frac{1}{2}}(\Delta v_{j+\frac{3}{2}} - 2\Delta v_{j+\frac{1}{2}} + \Delta v_{j-\frac{1}{2}}), \tag{29}$$

with

$$\Delta v_{j+\frac{1}{2}} = v_{j+1} - v_j.$$

Let $a_{j+\frac{1}{2}}$ be the numerically estimated wave speed

$$a_{j+\frac{1}{2}} = \begin{cases} \dfrac{f_{j+1} - f_j}{v_{j+1} - v_j}, & v_{j+1} \neq v_j, \\ \left.\dfrac{\partial f}{\partial u}\right|_{u=v_j}, & v_{j+1} = v_j, \end{cases}$$

as before. Then we have the following.

Theorem: The JST scheme is LED if whenever v_j or v_{j+1} is an extremum

$$\epsilon^{(2)}_{j+\frac{1}{2}} \geq \frac{1}{2}|a_{j+\frac{1}{2}}|, \quad \epsilon^{(4)}_{j+\frac{1}{2}} = 0 \tag{30}$$

Proof: Suppose v_j is an extremum. Then the second condition ensures that

$$\epsilon^{(4)}_{j+\frac{1}{2}} = 0, \quad \epsilon^{(4)}_{j-\frac{1}{2}} = 0.$$

Hence the scheme reduces to the 3 point scheme

$$\Delta x\frac{dv_j}{dt} = (\epsilon^{(2)}_{j+\frac{1}{2}} - \frac{1}{2}\alpha_{j+\frac{1}{2}})\Delta v_{j+\frac{1}{2}} - (\epsilon^{(2)}_{j-\frac{1}{2}} + \frac{1}{2}\alpha_{j-\frac{1}{2}})\Delta v_{j-\frac{1}{2}},$$

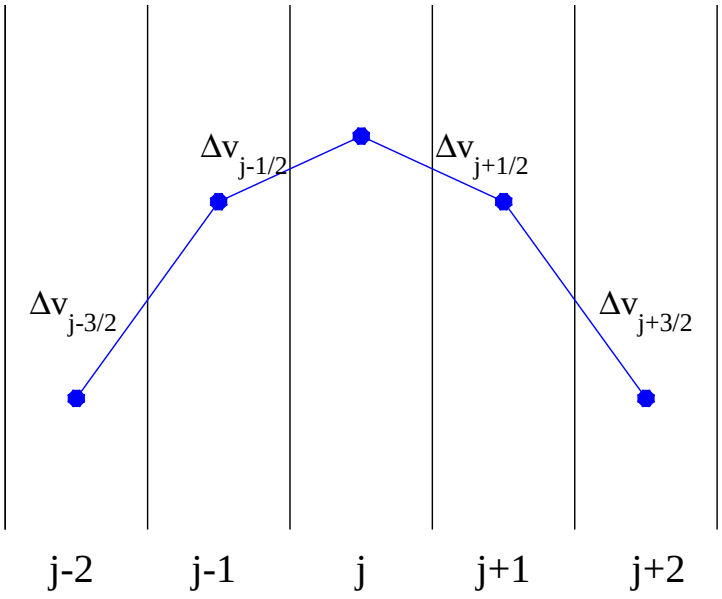

Figure 23: JST scheme at an extremum. $\Delta v_{j+\frac{3}{2}}$ and $\Delta v_{j-\frac{1}{2}}$ have opposite signs. Also $\Delta v_{j+\frac{1}{2}}$ and $\Delta v_{j-\frac{3}{2}}$ have opposite signs. Thus, $\epsilon^{(4)}_{j+\frac{1}{2}} = 0$ and $\epsilon^{(4)}_{j-\frac{1}{2}} = 0$.

and according to the first condition the coefficients of both $v_{j+1} - v_j$ and $v_{j-1} - v_j$ are non-negative, satisfying the requirements for an LED scheme.

In order to construct coefficients $\epsilon^{(2)}_{j+\frac{1}{2}}$ and $\epsilon^{(4)}_{j+\frac{1}{2}}$ satisfying conditions (30), define the function

$$R(u,v) = \left| \frac{u-v}{|u|+|v|} \right|^q,$$

where $q \geq 1$. Then, if u and v have opposite signs

$$R(u,v) = 1$$

Now set

$$\epsilon^{(2)}_{j+\frac{1}{2}} = \alpha_{j+\frac{1}{2}} Q_{j+\frac{1}{2}}$$

and

$$\epsilon^{(4)}_{j+\frac{1}{2}} = \beta_{j+\frac{1}{2}} (1 - Q_{j+\frac{1}{2}})$$

where

$$Q_{j+\frac{1}{2}} = R(\Delta v_{j+\frac{3}{2}}, \Delta v_{j-\frac{1}{2}})$$

Since $\Delta v_{j+\frac{3}{2}}$ and $\Delta v_{j-\frac{1}{2}}$ have opposite signs if either v_j or v_{j+1} is an extremum, the scheme will be LED if

$$\alpha_{j+\frac{1}{2}} \geq \frac{1}{2} |a_{j+\frac{1}{2}}|$$

Typically

$$\beta_{j+\frac{1}{2}} = \kappa_4 |a_{j+\frac{1}{2}}|$$

where in the case of steady state calculations κ_4 can be tuned to maximize the rate of convergence to a steady state.

This realization of the JST scheme is actually an example of a symmetric TVD scheme. Extremely similar symmetric TVD schemes were proposed by the author[24] and Yee[28]. These schemes obtain second order accuracy by subtracting an anti-diffusive term based on neighboring values to cancel the first order diffusive term, but limit the anti-diffusion in the vicinity of extrema to preserve the LED property. This idea was first introduced in the flux corrected transport (FCT) scheme proposed by Boris and Brook[9]. Their formulation used two stages. The first stage consisted of a first order accurate positive scheme. The second stage added negative diffusion to cancel the first order error, subject to a limit on its magnitude at any location where it would cause the appearance of a new extremum in the solution. In the symmetric limited positive (SLIP) scheme[29], which was a refinement of earlier symmetric TVD schemes, this is accomplished with a single stage.

The formulation is based on the concept of limited averages. A limited average $L(u,v)$ of u and v is defined as an average with the following properties.

- P1: $L(u,v) = L(v,u)$
- P2: $L(\alpha u, \alpha v) = \alpha L(u,v)$
- P3: $L(u,u) = u$
- P4: $L(u,v) = 0$ if u and v have opposite signs; otherwise $L(u,v)$ has the sign as u and v; or the same sign as whichever is nonzero if $u = 0$ or $v = 0$

The first three properties are satisfied by the arithmetic average. It is the fourth property that distinguishes the limited average.

In order to give some examples of limited averages, define

$$S(u,v) = \frac{1}{2} (\text{sgn}\,(u) + \text{sgn}\,(v))$$

so that

$$S(u,v) = \begin{cases} 1 & \text{when } u > 0 \text{ and } v > 0 \\ 0 & \text{when u and v have opposite sign} \\ -1 & \text{when } u < 0 \text{ and } v < 0 \end{cases}$$

Some well known limited averages are

- Minmod: $L(u,v) = S(u,v)\min(|u|,|v|)$
- Van Leer: $L(u,v) = S(u,v)2\frac{|u||v|}{|u|+|v|}$
- Superbee: $L(u,v) = S(u,v)\max\{\min(2|u|,|v|),\min(|u|,2|v|)\}$

Limited averages can be characterized by the function

$$\phi(r) = L(1,r) = L(r,1)$$

and it follows from properties P1 - P4 that

$$\phi(r) = 0, \quad r < 0,$$

$$\phi(r) \geq 0, \quad r \geq 0.$$

In the SLIP scheme, the diffusive flux is defined as

$$d_{j+\frac{1}{2}} = \alpha_{j+\frac{1}{2}}\left(\Delta v_{j+\frac{1}{2}} - L\left(\Delta v_{j+\frac{3}{2}}, \Delta v_{j-\frac{1}{2}}\right)\right)$$

and it can then be proved[29] that the resulting scheme is an LED scheme. In comparison with upwind TVD constructions, which require a limit $\phi(r) \leq 2$ as $r \to \infty$, there is no upper limit on $\phi(r)$.

A general class of limiters satisfying conditions P1 - P4 can be constructed as the arithmetic average multiplied by a switch:

$$L(u,v) = \frac{1}{2}D(u,v)(u+v)$$

where $0 \leq D(u,v) \leq 1$ and $D(u,v) = 0$ if u and v have opposite signs This is realized by the formula

$$D(u,v) = 1 - \left|\frac{u-v}{u+v}\right|^q$$

where q is a positive integer. This definition contains some of the previously defined limiters as follows:

$$q = 1 \text{ gives Minmod}$$

$$q = 2 \text{ gives the Van Leer limiter since } \frac{1}{2}\left(1 - \left|\frac{u-v}{u+v}\right|^2\right)(u+v) = \frac{2uv}{u+v}$$

As $q \to \infty, L(u,v)$ approaches a limit set by the arithmetic mean if u and v have the same sign and zero if they have opposite signs. The corresponding switch $\phi(r) = L(1,r)$ is illustrated in figure 24.

With this class of limiters the SLIP scheme recovers a variant of the JST scheme since

$$D(u,v) = 1 - R(u,v)$$

where $R(u,v)$ is the switch used in the JST scheme. Set

$$Q_{j+\frac{1}{2}} = R(\Delta v_{j+\frac{3}{2}}, \Delta v_{j-\frac{1}{2}})$$

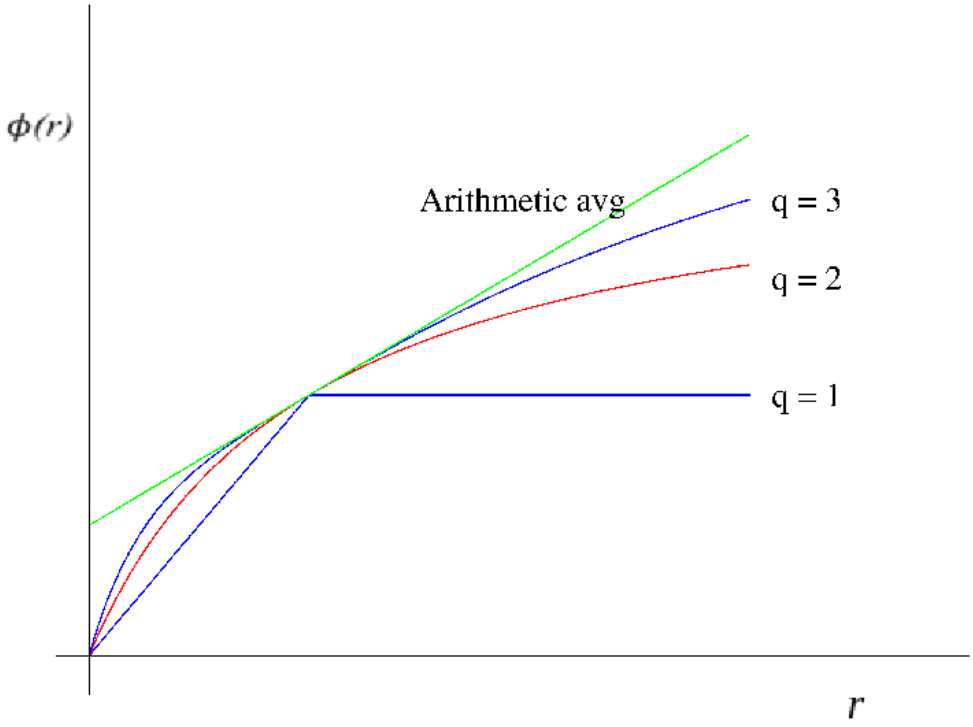

Figure 24: Switch ϕ as a function of r and q

Then the SLIP scheme can be written as

$$\begin{aligned} d_{j+\frac{1}{2}} &= \alpha_{j+\frac{1}{2}} \left\{ \Delta v_{j+\frac{1}{2}} - \frac{1}{2}(1 - Q_{j+\frac{1}{2}})(\Delta v_{j+\frac{3}{2}} + \Delta v_{j-\frac{1}{2}}) \right\} \\ &= \alpha_{j+\frac{1}{2}} Q_{j+\frac{1}{2}} \Delta v_{j+\frac{1}{2}} - \frac{1}{2}\alpha_{j+\frac{1}{2}}(1 - Q_{j+\frac{1}{2}})(\Delta v_{j+\frac{3}{2}} - 2\Delta v_{j+\frac{1}{2}} + \Delta v_{j-\frac{1}{2}}) \end{aligned}$$

This is the JST scheme with $\kappa_4 = \dfrac{1}{2}$.

It may also be noted that the SLIP scheme may be reformulated as a second order accurate reconstruction scheme in which the left and right states at the interface $j + \frac{1}{2}$ are set equal to

$$w_L = w_j + \frac{1}{2} L \left(\Delta w_{j+\frac{3}{2}}, \Delta w_{j-\frac{1}{2}} \right)$$

and

$$w_R = w_j - \frac{1}{2} L \left(\Delta w_{j+\frac{3}{2}}, \Delta w_{j-\frac{1}{2}} \right)$$

so that

$$w_R - w_L = \Delta w_{j+\frac{1}{2}} - L \left(\Delta w_{j+\frac{3}{2}}, \Delta w_{j-\frac{1}{2}} \right).$$

Then, a scheme with scalar diffusion is recovered by setting

$$d_{j+\frac{1}{2}} = \alpha_{j+\frac{1}{2}} (w_R - w_L).$$

On the other hand, any two point flux function $f(w_R, w_L)$ may be used as the interface flux. In this manner, the SLIP scheme can be combined with the Roe flux, or, for example, the author's E- and H-CUSP schemes, and it has proven to be very robust. Figure 25 shows a transonic flow solution using SLIP reconstruction with the Roe flux while figure 26 shows a solution for the flow over a blunt body at Mach 8 using SLIP reconstruction with the H-CUSP flux developed by the author[30]. A slight modification of the SLIP scheme which recovers the whole range of JST schemes with an arbitrary choice of κ_4 is to set

$$d_{j+\frac{1}{2}} = \alpha_{j+\frac{1}{2}} \left(\Delta w_{j+\frac{1}{2}} - A_{j+\frac{1}{2}} \right),$$

where

$$A_{j+\frac{1}{2}} = \left(1 - Q_{j+\frac{1}{2}} \right) \left((1 - 2\kappa_4) \Delta w_{j+\frac{1}{2}} + \kappa_4 \left(\Delta w_{j+\frac{3}{2}} + \Delta w_{j-\frac{1}{2}} \right) \right).$$

This can also be reformulated as a second order accurate reconstruction scheme. Thus, the JST scheme can be used as a reconstruction procedure in conjunction with any two point flux formula.

VI. Time dependent problems

While the primary goal of the JST scheme was the solution of steady state problems, it can also be used directly for time dependent simulations provided that the same time step is used throughtout the domain. In this case, the multigrid time stepping procedure should not be used, and the additive Runge-Kutta schemes described in Sections II. and III. are not appropriate. Instead, one should use the standard fourth order Runge-Kutta scheme:

$$\begin{aligned} w^{(1)} &= w^{(0)} - \frac{1}{2}\Delta t R(w^{(0)}), \\ w^{(2)} &= w^{(0)} - \frac{1}{2}\Delta t R(w^{(1)}), \\ w^{(3)} &= w^{(0)} - \Delta t R(w^{(2)}), \\ w^{(4)} &= w^{(0)} - \frac{1}{6}\Delta t \left(R(w^{(0)}) + 2R(w^{(1)}) + 2R(w^{(2)}) + R(w^{(3)}) \right). \end{aligned}$$

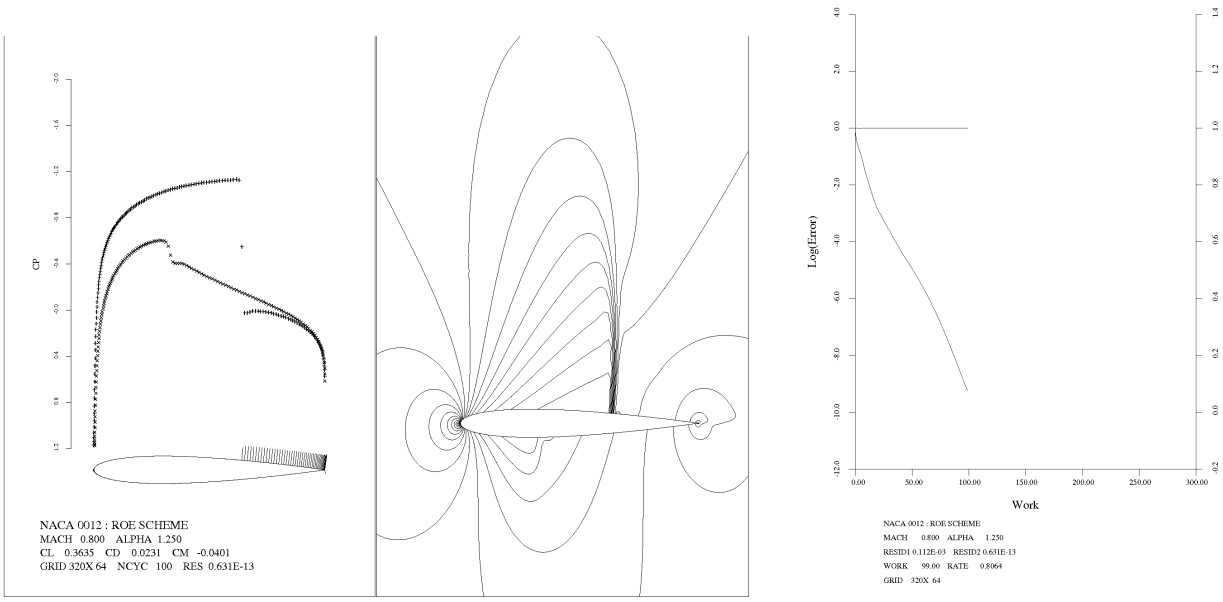

(a) (b)

Figure 25: NACA 0012: Roe flux with SLIP reconstruction and symmetric Gauss-Seidel multigrid scheme.

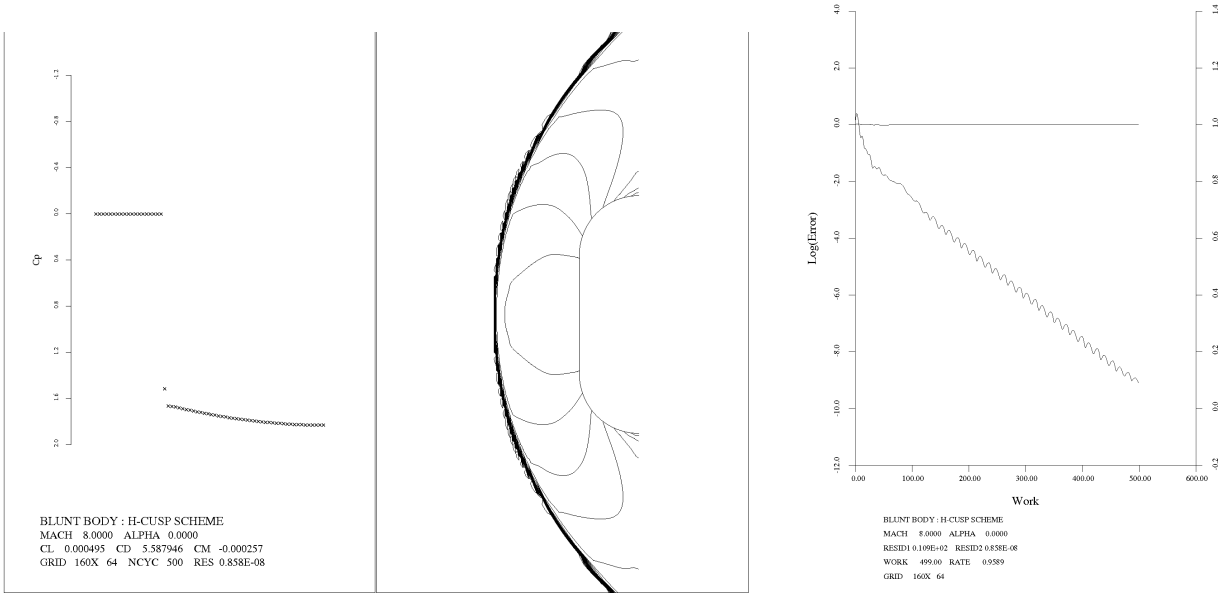

(a) (b)

Figure 26: Blunt body: H-CUSP scheme.

In the case of a flow with moving shock waves, one may prefer to use one of the strong stability preserving (SSP) Runge-Kutta schemes developed during the last two decades by Shu, Gottlieb and others[31]. These schemes can be expressed as convex combinations of forward Euler steps, and consequently, as long as the time step is appropriately restricted, they preserve strong stability properties, such as the TVD property, whenever the forward Euler discretization has these properties. An attractive choice is the Shu-Osher scheme[32].

$$\begin{aligned} w^{(1)} &= w^{(0)} - \Delta t R\left(w^{(0)}\right), \\ w^{(2)} &= \frac{3}{4}w^{(0)} + \frac{1}{4}\left(w^{(1)} - \Delta t R(w^{(1)}\right), \\ w^{(3)} &= \frac{1}{3}w^{(0)} + \frac{2}{3}\left(w^{(2)} - \Delta t R(w^{(2)}\right), \end{aligned}$$

which is third order accurate and SSP for CFL numbers ≤ 1.

Figure 27 shows the results of a shock tube calculation for the well known Sod test case[33] using the JST scheme in conjunction with the Shu-Osher time stepping scheme at a CFL number of unity. For this calculation, the sensor was based on the density in order to detect the contact discontinuity. Setting

$$r = \frac{\left|\Delta\rho_{j+\frac{1}{2}} - \Delta\rho_{j-\frac{1}{2}}\right|}{\max\left(\left(\left|\Delta\rho_{j+\frac{1}{2}}\right| + \left|\Delta\rho_{j-\frac{1}{2}}\right|\right), \rho_{\lim}\right)},$$

$$s_j = r^2,$$

so that it scales $\mathcal{O}(\Delta x^2)$ in smooth regions, while the JST constants were $\kappa_2 = 1$, $\kappa_4 = \frac{1}{32}$ and $c_4 = 4$.

VII. Viscous flows

The JST scheme has proven quite successful for viscous compressible flows modeled by the Reynolds averaged Navier-Stokes (RANS) equations. A major obstacle to obtaining fast convergence to a steady state is the need to compress the mesh in the boundary layer towards the wall, so that the height of the first mesh cell is $\approx y^+ = 1$ measured in viscous wall units. These results in very high aspect ratio cells near the wall. Here the flexibility of the JST scheme proves helpful. In the doctoral research of Martinelli[34], it was found that convergence could be improved by rescaling the spectral radii in the i and j coordinate directions. Suppose that these are r_i and r_j respectively. Then setting $a = r_i$, we scale $\epsilon^{(2)}$ and $\epsilon^{(4)}$ in the i and j coordinate directions to

$$\tilde{r}_i = r_i\left(1 + \frac{1}{a}\right)^{\beta}$$

and

$$\tilde{r}_j = r_j\left(1 + a\right)^{\beta},$$

where it has been found by numerical experimentation that a good choice for the exponent is $\beta = 2/3$.

Multigrid RANS calculations using Runge-Kutta schemes generally exhibit fast convergence of the residual by around three orders of magnitude over the first 50 steps, but slow asymptotic convergence after that. Nevertheless, the lift and drag coefficients are usually converged to four digits in around 300 steps. Recently the author has been able to obtain sustained fast convergence with a hybrid Runge-Kutta symmetric Gauss-Seidel (RKSGS) scheme along the lines suggested by Rossow[36] and Swanson, Turkel and Rossow[37]. In this scheme, the corrections are modified by a preconditioner which uses a single double sweep of a symmetric LUSGS scheme at each Runge-Kutta stage. As in the additive Runge-Kutta scheme, the diffusive part of the residual (both the true viscous terms and the added dissipative terms) is under-relaxed at each stage, while the preconditioned solution is over-relaxed. This time integration scheme seems to be particularly effective when it is combined with the JST scheme.

Figure 28 shows the results for the RAE 2822, Case 9, calculated on a 512×64 C-mesh. In this calculation, the residual was reduced 13 orders of magnitude in 100 multigrid W-cycles, with a mean convergence rate of 0.7446. The

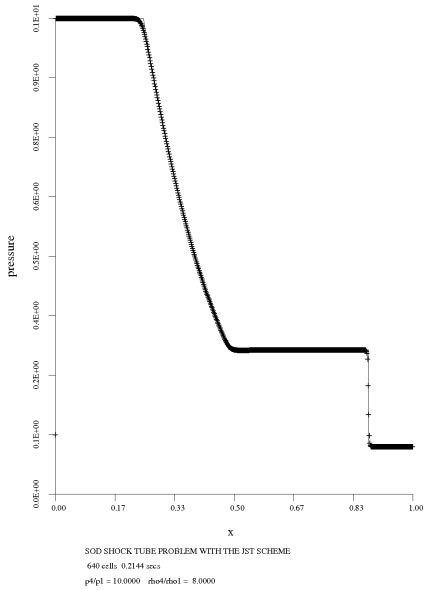

Pressure

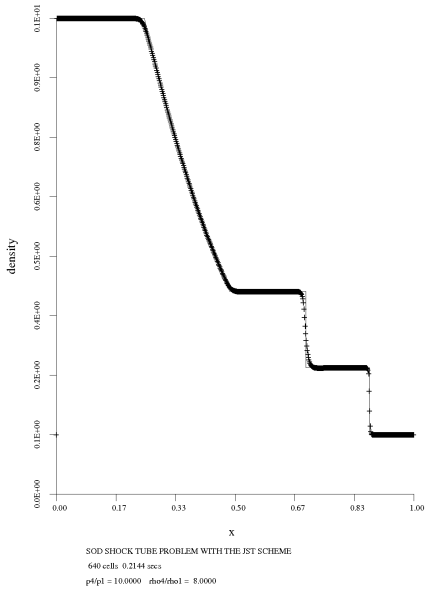

Density

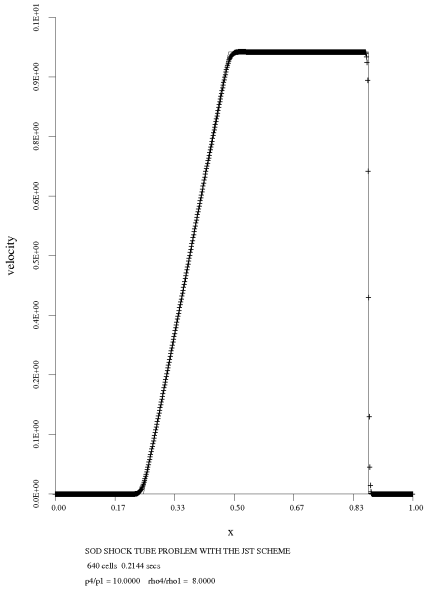

Velocity

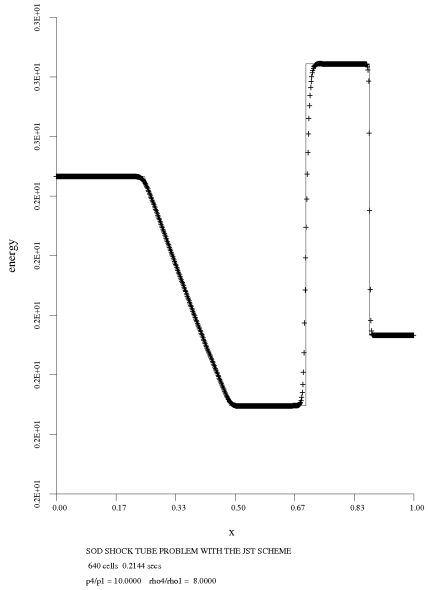

Energy

Figure 27: Sod shock tube problem with the JST scheme: 640 cells

additive RK scheme had two stages with coefficients

$$\alpha_1 = 0.24, \quad \alpha_2 = 1,$$

and

$$\beta_1 = 1, \quad \beta_2 = 2/3,$$

in the notation of section III.. The over-relaxation factor for the preconditiner was $1/0.65$ on both fine and coarse grids.

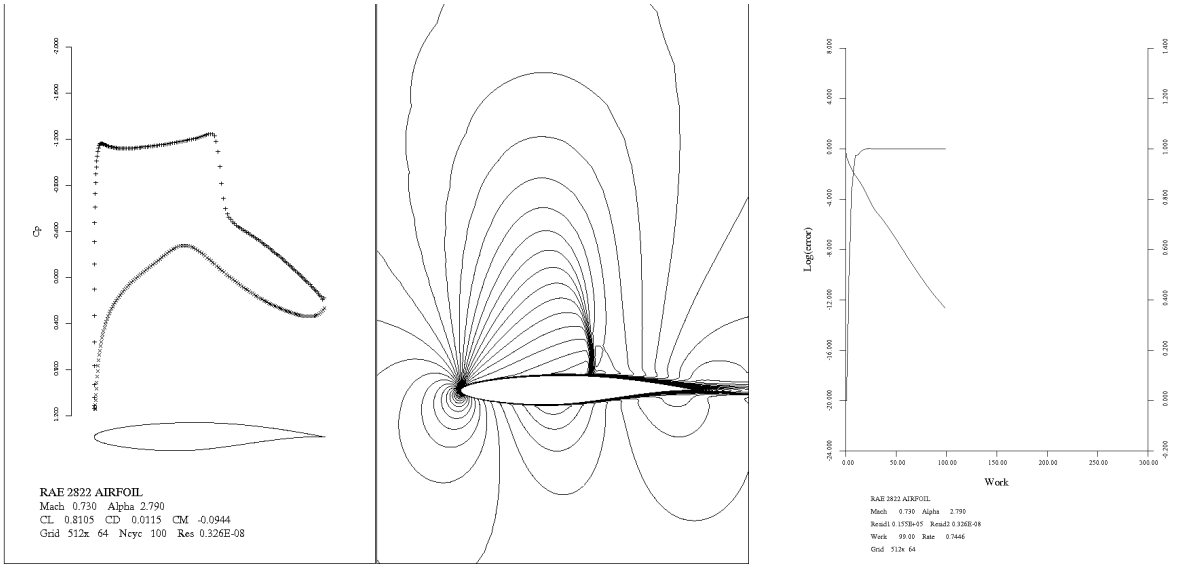

(a) (b)

Figure 28: RAE 2822, Case 9; $M = 0.73$, $\alpha = 2.79°$.

VIII. Conclusion

The JST scheme has had a longevity which was unanticipated (at least by the author). It is probably fair to say that it was the first numerical scheme for the Euler equations which reliably produced non-oscillatory solutions for flows with shock waves, and also reliably converged to a steady state. As a more complete theory for the design of high resolution shock capturing schemes emerged, it became apparent that the JST scheme could easily be reformulated as a TVD scheme. It also proved to be easily extendable to unstructured meshes, and it seems to be one of the preferred options in Stanford's SU2 software and the German Tau code. It has recently been found that very fast steady state RANS solutions approaching "textbook" multigrid convergence rates, can be realized when the JST scheme is used in conjunction with an RKSGS time integration scheme. The JST scheme has also proved to be a competitive discretization scheme for problems in solid mechanics. Figure 29 shows the response of a beam to a lateral impact calculated by the JST scheme[38].

The JST scheme has certainly contributed to the development of second order accurate high resolution shock capturing schemes. However, in the last decade, CFD has been on a plateau where RANS simulations have been performed for increasingly complex configurations and progressively finer meshes, now of the order of 100 million cells. These calculations cannot adequately simulate vortex dominated flows such as rotorcraft flows, because second order accurate discretizations introduce too much numerical dissipation, with the consequence that vortices get washed out before they have traveled any significant distance. Moreover, the behavior of unsteady separated and turbulent flows cannot be reliably predicted by the prevailing RANS methods, and in the long run, it seems likely that higher fidelity methods such

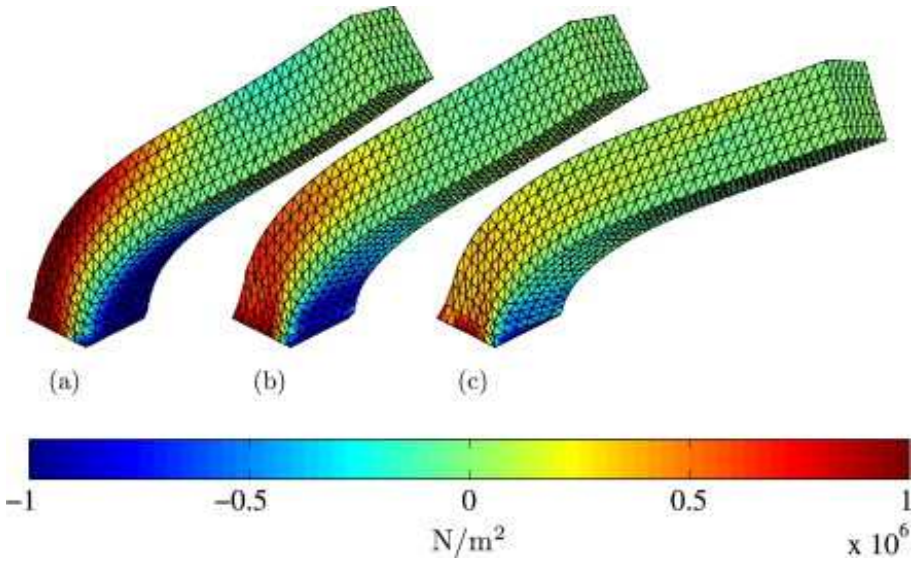

Figure 29: Three dimensional bending column. Initial uniform velocity $V_0 = 10(\cos(30), \sin(30), 0)^T$ m/s. Comparison of the pressure distribution for two different materials: hyperelastic constitutive model (a), von Mises hyperelastic plastic constitutive models (b), (c) at time $t = 0.45$ s. Young's modulus $E = 1.7 \times 10^7$ Pa, density $\rho_0 = 1.1 \times 10^3$ kg/m^3 and Poisson's ratio $\nu = 0.45$. Yield stress, $\bar{\tau}_y^0 = 2$ GPa (b), $\bar{\tau}_y^0 = 1$ GPa (c), hardening modulus $H = 0.5$ GPa. JST spatial discretisation with $h = 1/6$ m, $\kappa^{(4)} = 1/128$ and $\alpha_{\text{CFL}} = 0.4$. Source: Aguirre *et al.* [38].

as large eddy simulation (LES) must be used. The challenge moving forward, is to devise higher order methods with less numerical dissipation which can both track persistent vortices and also resolve a larger fraction of the scales in high Reynolds number turbulent flow simulations.

Acknowledgements

The author has benefited greatly from the mentoring of Paul Garabedian at the Courant Institute. During the early years of the development of the JST scheme, the research was supported in part by NASA and also the Office of Naval Research, originally under the oversight of Morton Cooper, and later under the oversight of Spiro Lekoudis.

References

[1]Harten, A., High resolution schemes for hyperbolic conservation laws, *J. Comp. Phys.*, Elsevier, 1983, Vol. 49, No. 3, 357-393.

[2]Roe, P. L., Approximate Riemann solvers, parameter vectors, and difference schemes, *J. Comp. Phys.*, 1981, Elsevier, 43, 357-372.

[3]Van Leer, B., Towards the ultimate conservative difference scheme I. The quest of monotonicity, *Proceedings of the Third International Conference on Numerical Methods in Fluid Mechanics*, 163-168, 1973.

[4]Van Leer, B., Towards the ultimate conservative difference scheme. II. Monotonicity and conservation combined in a second order scheme, *J. Comp. Phys.*, 1974, 14, 361-370.

[5]Van Leer, B., Towards the ultimate conservative difference scheme III. Upstream-centered finite-difference schemes for ideal compressible flow, *J. Comp. Phys.*, Elsevier, 1977, 23, 263-275.

[6]Van Leer, B., Towards the ultimate conservative difference scheme. IV. A new approach to numerical convection, *J. Comp. Phys.*, Elsevier, 1977, 23, 276-299.

[7]Van Leer, B., Towards the ultimate conservative difference scheme. V. A second-order sequel to Godunov's method, *J. Comp. Phys.*, Elsevier, 1979, 32, 101-136.

[8]Godunov, S. K., A Difference Method for the Numerical Calculation of Discontinuous Solutions of Hydrodynamic Equations, *Mat. Sbornik*, 1959, 47, 271-306.

[9]Boris, J. P. & Book, D. L., Flux-corrected transport. I. SHASTA, A fluid transport algorithm that works, *J. Comp. Phys.*, Elsevier, 1973, 11, 38-69.

[10]Jameson, A., Numerical Calculations of the Three-Dimensional Transonic Flow Over a Yawed Wing, *Proceedings of the AIAA Computational Fluid Dynamics Conference*, Palm Springs, July 1973, pp. 18-26.

[11]Jameson, A., Caughey, D., Newman, P. & Davis, R., A Brief Description of the Jameson Caughey NYU Transonic Swept-Wing Computer Program *FLO22*, *NASA Technical Memorandum*, NASA TM X-73996, December 1976.

[12]Jameson, A. & Caughey, D. A., A Finite Volume Method for Transonic Potential Flow Calculations, *Proc. AIAA 3rd Computational Fluid Dynamics Conference*, 1977, 35-54.

[13]Bristeau, M. O.; Glowinski, R.; Periaux, J.; Perrier, P.; Poirier, G. & Pironneau, O., Transonic flow simulations by finite elements and least square methods, *Proceedings of the 3rd International Conference on Finite Elements in Flow Problems*, Banff, Alberta, Canada, 1981, 11-29.

[14]MacCormack, R. W., The Effect of Viscosity in Hypervelocity Impact Cratering, AIAA Paper 69-354, 1969.

[15]Jameson, A. & Turkel, E., Implicit schemes and LU decompositions, *Mathematics of Computation*, Wiley, 1981, 37, 385-397.

[16]MacCormack, R. W., A numerical method for solving the equations of compressible viscous flow, *AIAA Journal*, 1982, 20, 1275-1281

[17]Rusanov, V. V., Calculation of interaction of non-steady shock waves with obstacles, *J. Comput. Math. Phys. USSR*, NRC, Division of Mechanical Engineering, 1961, 267-279.

[18]Cooper, G. J. & Sayfy, A., Additive methods for the numerical solution of ordinary differential equations, *Mathematics of Computation*, 1980, 35, 1159-1172.

[19]Cooper, G. J. & Sayfy, A., Additive Runge-Kutta methods for stiff ordinary differential equations, *Mathematics of Computation*, 1983, 40, 207-218.

[20]Busch Jr., R. J., Computational Fluid Dynamics in the Design of the Northrop/McDonnell Douglas YF-23 ATF Prototype, AIAA paper 91-1627, AIAA 21st Fluid Dynamics, Plasmadynamics & Lasers Conference, 1991.

[21]Jameson, A. & Baker, T. J., Solution of the Euler Equations for Complex Configurations, *Proc. AIAA 6th Computational Fluid Dynamics Conference*, Denvers, 1983, 293-302.

[22]Ni, R. H. A Multiple Grid Scheme for Solving the Euler Equations, *AIAA Journal*, 1982, 20, 1565-1571.

[23]Martinelli, L. & Jameson, A., Validation of a Multigrid Method for the Reynolds Averaged Equations, AIAA Paper 88-0414, AIM 26th Aerospace Sciences Meeting January 11-14, 1988, Reno, Nevada.

[24]Jameson, A., Transonic Flow Calculations for Aircraft, *Lecture Notes in Mathematics, Numerical Methods in Fluid Dynamics*, Brezzi, F. (Ed.) , Springer Verlag, 1985, 156-242.

[25]Jameson, A., Baker, T. J. & Weatherill, N. P., Calculation of Inviscid Transonic Flow over a Complete Aircraft, AIAA Paper 86-0103, AIAA 24th Aerospace Sciences Meeting, 1986.

[26]Vijayasundaram, G., Transonic flow simulations using an upstream centered scheme of Godunov in finite elements, *Journal of Computational Physics*, Elsevier, 1986, 63, 416-433.

[27]Jameson, A., *AA215 A & B Lecture Notes, Advanced Computational Fluid Dynamics*, Stanford University.

[28]Yee, H. C., On Symmetric and Upwind TVD Schemes, *Proc. 6th GAMM Conference on Numerical Methods in Fluid Mechanics*, 1985.

[29]Jameson, A., Artificial Diffusion, Upwind Biasing, Limiters and their Effect on Accuracy and Multigrid Convergence in Transonic and Hypersonic Flows, AIAA Paper 93-3359, AIAA 11th Computational Fluid Dynamics Conference, Orlando, 1993.

[30]Jameson, A., Analysis and Design of Numerical Schemes for Gas Dynamics 2, Artificial Diffusion and Discrete Shock Structure, *Int. J. of Comp. Fluid Dyn.*, 1995, 5, 1-38.

[31]Gottlieb, S. & Shu, C.-W., Total variation diminishing Runge-Kutta schemes, *Mathematics of Computation of the American Mathematical Society*, 1998, 67, 73-85.

[32]Shu, C. W. & Osher, S., Efficient Implementation of Essentially Non-Oscillatory Shock-Capturing Schemes, *J. Comp. Phys.*, 1988, 77, 439-471.

[33]Sod, G. A., A survey of several finite difference methods for systems of nonlinear hyperbolic conservation laws, *Journal of Computational Physics*, Elsevier, 1978, 27, 1-31.

[34]Martinelli, L., Calculations of Viscous Flows with a Multigrid Method, *Princeton University Thesis*, 1987.

[35]Yakhot, V. & Orszag, S. A., Renormalization Group Analysis of Turbulence. I. Basic Theory, *J. Sci. Comp.*, 1986, 1, 3-51.

[36]Rossow, C.-C., Efficient computation of compressible and incompressible flows, *Journal of Computational Physics*, Elsevier, 2007, 220, 879-899.

[37]Swanson, R., Turkel, E. & Rossow, C.-C., Convergence acceleration of Runge–Kutta schemes for solving the Navier-Stokes equations, *Journal of Computational Physics*, Elsevier, 2007, 224, 365-388.

[38]Aguirre, M., Gil, A. J., Bonet, J. & Carreo, A. A., A vertex centred finite volume Jameson-Schmidt-Turkel (JST) algorithm for a mixed conservation formulation in solid dynamics, *Journal of Computational Physics*, Elsevier, 2014, 259, 672-699.